High-resolution inelastic electron scattering from ^{17}O

D. M. Manley[a]

Lawrence Livermore National Laboratory, University of California, Livermore, California 94550
and Department of Physics, Kent State University, Kent, Ohio 44242

B. L. Berman

Lawrence Livermore National Laboratory, University of California, Livermore, California 94550
and Department of Physics, The George Washington University, Washington, D.C. 20052

W. Bertozzi, T. N. Buti,[b] J. M. Finn,[c] F. W. Hersman,[d] C. E. Hyde-Wright,[e] M. V. Hynes,[f]
J. J. Kelly,[g] M. A. Kovash,[h] S. Kowalski, R. W. Lourie, B. Murdock,[i] B. E. Norum,[j]
B. Pugh,[h] and C. P. Sargent[k]

Department of Physics and Laboratory for Nuclear Science, Massachusetts Institute of Technology,
Cambridge, Massachusetts 02139

(Received 30 January 1987)

Excited states of ^{17}O up to an excitation energy of 15 MeV have been studied by high-resolution electron scattering for momentum transfers between 0.8 and 2.6 fm^{-1}. Previous electron-scattering measurements in this excitation region were confined to momentum transfers below 1.1 fm^{-1} and were of lower resolution. Form factors were measured and reduced transition probabilities determined for most excited states below 9.5 MeV. The present data are interpreted within the framework of weak-coupling models to facilitate a simple description of the observed spectrum. Particular emphasis is placed upon understanding states that are excited strongly by electric quadrupole or octupole transitions. Spins and parities have been assigned for several levels that have very narrow widths and, hence, are not amenable to partial-wave analyses involving the ^{16}O+n and ^{13}C+α reactions. Levels at 5.87 MeV ($\frac{3}{2}^+$), 6.86 MeV ($\frac{5}{2}^+$), 7.58 MeV ($\frac{7}{2}^+$), and 8.47 MeV ($\frac{9}{2}^+$) are suggested as candidates for predominantly 5p-4h members of a $K^\pi = \frac{3}{2}^+$ rotational band. A narrow state ($\Gamma \leq 20$ keV) at 12.22±0.02 MeV was observed for the first time and the existence of narrow states at 8.90±0.02 and 14.72±0.02 MeV was confirmed.

I. INTRODUCTION

^{17}O is known[1] to have approximately 45 excited states below 10 MeV of excitation. This oxygen isotope therefore presents a challenging opportunity in which to understand a rich level structure in a light, stable nucleus. (A level diagram for the known states up to an excitation energy of 15 MeV is shown in Fig. 1.) Virtually all prior information concerning spins and parities of levels below 15 MeV was obtained from partial-wave analyses of the ^{16}O + n and ^{13}C+α reactions. Most low-lying levels are amenable to such studies because the thresholds for ^{17}O to decay by neutron and alpha emission are relatively low (4.14 and 6.36 MeV, respectively). Of the three excited states below the neutron-decay threshold, the level at 0.87 MeV was identified to be the "single-particle" $\frac{1}{2}^+$ state from a study[2] of the ^{16}O(d,p)^{17}O stripping reaction and the levels at 3.06 and 3.84 MeV were identified to have $J^\pi = \frac{1}{2}^-$ and $\frac{5}{2}^-$, respectively, from a coincidence study[3] of the ^{14}C(α,nγ)^{17}O reaction.

The differential cross section (at 98°) for the ^{17}O(γ,n$_0$)^{16}O reaction was measured for the first time by Johnson et al.[4] in their investigation of excited states of ^{17}O with real photons. At least 30 states between 5 and 33 MeV of excitation were observed. This reaction is sensitive mainly to $T = \frac{1}{2}$ states that are excited strongly by E1 transitions. Experimental studies also have been performed (see Ref. 1 and references therein) involving many other reactions, some of which selectively excite states dominated by special configurations. The present work is a spectroscopic study of ^{17}O by inelastic electron scattering.

The first study of ^{17}O by inelastic electron scattering was performed by Kim et al.[3] at momentum transfers between 0.6 and 1.1 fm^{-1}. Although all states below 9 MeV of excitation were investigated, levels closer than 120 keV were not individually resolved. The giant resonance region of ^{17}O also has been investigated[6] by low-resolution inelastic electron scattering at momentum transfers between 0.34 and 0.98 fm^{-1}. Recently, $T = \frac{3}{2}$ levels in ^{17}O between excitation energies of 11 and 15.3 MeV were studied by a high-resolution electron-scattering experiment[7] at momentum transfers between 0.32 and 0.52 fm^{-1}.

The present work reports the first measurements of inelastic electron scattering from ^{17}O for states below 15 MeV at momentum transfers above 1.1 fm^{-1}. High-resolution measurements were performed at the MIT-Bates Linear Accelerator Center, primarily at 90° and 160°, for momentum transfers between 0.8 and 2.6 fm^{-1}.
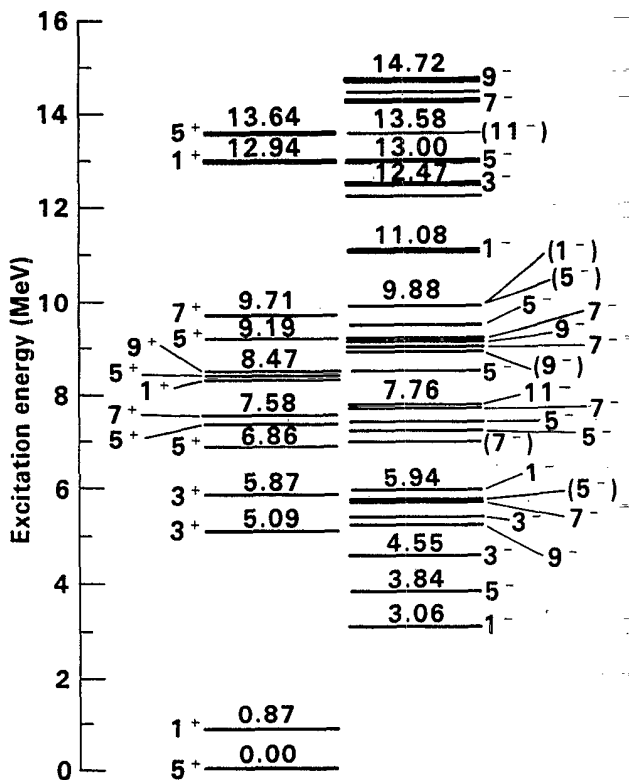
FIG. 1. Experimental level diagram for ^{17}O. States are labeled by $2J^\pi$ and, in most cases, by their excitation energy. Most states with widths greater than 40 keV are not shown. Above 9.5 MeV, only $T = \frac{3}{2}$ states (heavy lines) and states seen in the present experiment are included.

Limited measurements, which are reported elsewhere,[8] also were performed for states between 15 and 23 MeV. Form factors were extracted for most states below 9.5 MeV and for the more strongly excited narrow states between 9.5 and 15 MeV. The deduced electromagnetic decay properties of these levels, when combined with information from other experiments and from nuclear-structure calculations, allow spins and parities to be assigned for several narrow levels (typically, $\Gamma \lesssim 2$ keV) that previously had either unknown or questionable spins and/or parities. In some cases, prior tentative J^π assignments have been confirmed. This work therefore provides a major step toward understanding the low-lying level structure of ^{17}O.

The remainder of this paper presents detailed descriptions of the measured form factors for individual excited states and our interpretations of the states in terms of simple nuclear-structure models. Comparisons will be made, when possible, to selected shell-model calculations. The experimental details of the present measurements are discussed in Sec. II. The data analysis, which encompasses extraction of cross sections and form factors from the measured electron energy-loss spectra, separation of the form factors into longitudinal and transverse components, and decomposition of the longitudinal and transverse form factors into contributions from individual multipoles, is discussed in Sec. III. A review of the weak-coupling model for particles and holes is

presented in Sec. IV. Several low-lying levels in ^{16}O and ^{17}O are described and compared. Detailed results for individual states are discussed in Sec. V. Information from several earlier experiments is reviewed and discussed, as appropriate, to elucidate the properties and structures of states observed in the present experiment. This section is divided into four parts. The first part discusses the "single-particle" positive-parity states at 0.87 and 5.09 MeV. The second part discusses the collective positive-parity states below 9.5 MeV of excitation. Emphasis is placed on describing members of a proposed $K^\pi = \frac{3}{2}^+$ rotational band, which are strongly excited by electric quadrupole transitions. The third part describes the negative-parity states below 9.5 MeV. Here the focus is on describing states with strong electric octupole transitions. The fourth and final part of Sec. V describes the states observed between 9.5 and 15 MeV. In this excitation region, many of the sharp states have $T = \frac{3}{2}$; thus, our high-momentum-transfer data complement the electron-scattering measurements of $T = \frac{3}{2}$ levels by Rangacharyulu et al.,[7] which were performed at low momentum transfers. The conclusions and main findings of the present work are summarized in Sec. VI.

II. EXPERIMENTAL DETAILS

The present electron-scattering measurements for ^{17}O were performed at the MIT-Bates Linear Accelerator Center as part of a comprehensive program to study the oxygen isotopes ^{16}O, ^{17}O, and ^{18}O. Our elastic-scattering measurements for these isotopes are discussed in Ref. 9, whereas our previous inelastic-scattering measurements are discussed in Refs. 10 and 11 for ^{16}O, Ref. 8 for ^{17}O, and Refs. 8 and 12 for ^{18}O. The MIT energy-loss spectrometer system (ELSSY) used for these measurements is described by Bertozzi et al.[13] General experimental details are described elsewhere.[10]

Spectra of scattered electrons were measured at 90° for incident electron energies of 119.4, 149.3, 174.8, 175.4, 194.3, 209.2, 228.3, 248.4, and 268.8 MeV, which correspond to momentum transfers (q) between 0.8 and 1.9 fm^{-1}. Spectra also were measured at 160° for incident electron energies of 100.5, 105.0, 115.3, 125.0, 139.7, 169.9, and 179.5 MeV ($1.0 \leq q \leq 1.8$ fm^{-1}) and at 140° for an incident energy of 134.2 MeV ($q = 1.3$ fm^{-1}). The energy resolution [full width at half maximum (FWHM)] for the measurements ranged from 20 to 50 keV at 90°, from 30 to 60 keV at 140°, and from 70 to 80 keV at 160°.

Form factors extracted from the present measurements were analyzed simultaneously with (unpublished) form factors from an earlier set of measurements.[12] Early measurements were performed at 90° for incident energies between 170.4 and 369.2 MeV ($1.2 \leq q \leq 2.6$ fm^{-1}) and at 160° for incident energies between 171.2 and 256.2 MeV ($1.7 \leq q \leq 2.6$ fm^{-1}). Form factors measured at 90° were available only for the levels at 0.87, 3.06, 3.84, 5.22, 5.38, 6.97, 7.17, and 7.76 MeV; form factors measured at 160° were available only for the level at 0.87 MeV.

A single ^{17}O target of average thickness 29.1 mg/cm^2 was used for all of the present measurements performed at 90° and 160°. A second ^{17}O target of average thickness 28.7 mg/cm^2 was used for the 140° measurements. Both targets were isotopically enriched BeO foils manufactured at Lawrence Livermore National Laboratory.[14] Details of their fabrication are described briefly in Ref. 12. Isotopic oxygen abundances relative to beryllium were approximately the same (within 1%) for both targets: 85% ^{17}O, 11% ^{16}O, and 4% ^{18}O. The determination of the relative abundances also is discussed in Ref. 12. The targets also contained impurities (absolute abundances were a few percent) from carbon and nitrogen. Background peaks from ^{9}Be, ^{16}O, and ^{18}O were taken into account by fitting spectra measured with targets of pure metallic beryllium and with BeO foils that contained either natural oxygen or were enriched in ^{18}O. Spectra obtained with these targets were measured under the same kinematic conditions as for the ^{17}O targets.

III. DATA ANALYSIS

A. Line-shape analysis

The procedures that were used to fit spectra and extract cross sections and the corresponding form factors will be reviewed here briefly; further details can be found elsewhere.[8,10] Spectra were fitted with a modified version of the MIT line-shape–fitting routine ALLFIT,[15] which uses a maximum-likelihood algorithm based upon Poisson statistics. This code parametrizes spectra by a sum of peak-shape functions and a background term.

The peak-shape function is described by a convolution of an instrumental resolution function, an intrinsic line-shape function, and a radiative response function. The form of the resolution function was taken to be a ten-parameter asymmetric hyper-Gaussian distribution with exponential tails.[11] One set of parameters was used to describe oxygen peaks and another set was used for beryllium peaks. In practice, good fits were obtained by suppressing the tail region and varying only the five parameters that describe the central part of the resolution function. The form of the intrinsic line-shape function was taken to be a Lorentzian distribution for peaks with $\Gamma > 10$ keV and a delta-function distribution for narrower peaks. The radiative response function was calculated following the theoretical work of Mo and Tsai,[16] as applied by Bergstrom[17] and Creswell.[18] Finally, the background term was described by a quadratic or lower-order polynomial in the electron energy loss, which was allowed to have a discontinuous increase in slope at the neutron-decay threshold of ^{9}Be.

The following procedure was used to handle background peaks from the ^{9}Be, ^{16}O, and ^{18}O contaminants. First, contributions from ^{9}Be peaks were determined by fitting the appropriate ^{9}Be spectrum. Next, contributions from ^{16}O peaks were extracted by fitting the corresponding ^{9}Be^{16}O spectrum and varying only an overall normalization factor to describe the ^{9}Be contribution. Contributions from ^{18}O peaks then were obtained by fitting the ^{9}Be^{18}O spectrum and accounting for contributions from ^{9}Be and ^{16}O in a similar manner. The only significant ^{17}O peaks in the ^{9}Be^{18}O spectra were those
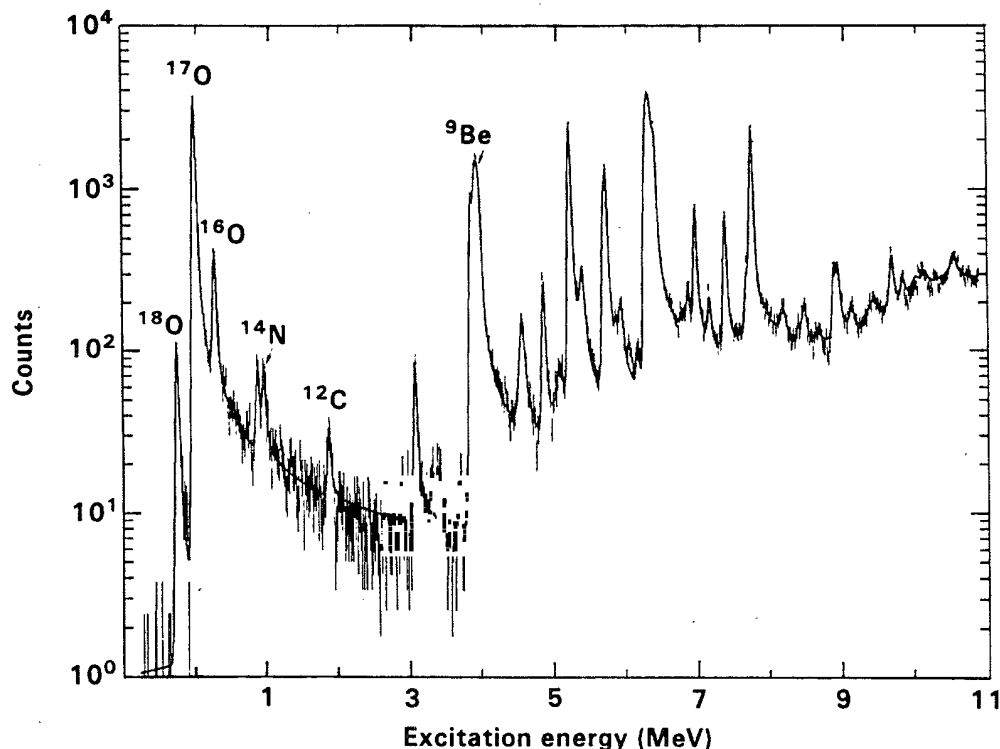

FIG. 2. Fitted electron spectrum for ^{9}Be^{17}O measured at $\theta = 90°$ for $E_0 = 268.8$ MeV. The curve shows the results of the overall fit, which had 73 peaks and 78 free parameters. Peaks are labeled for the ground states of ^{9}Be, ^{12}C, ^{14}N, ^{16}O, ^{17}O, and ^{18}O.
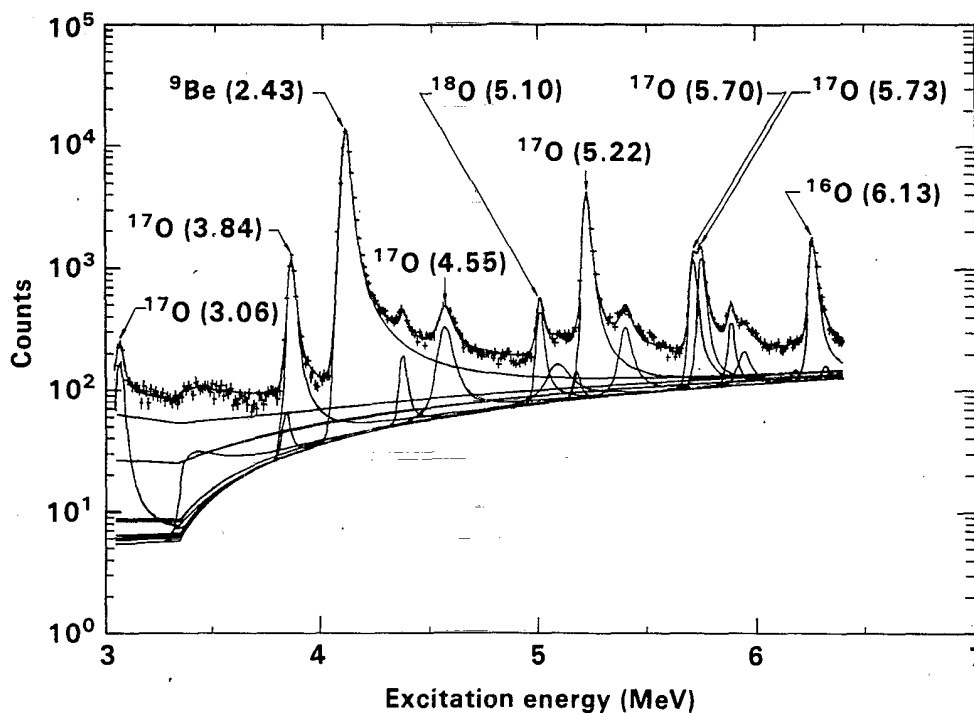
FIG. 3. Part of a fitted electron spectrum for ^{9}Be^{17}O measured at $\theta=90°$ for $E_0=174.8$ MeV. The curves show the results of both the overall fit and contributions from individual peaks. The entire fitted spectrum extended from 0 to 6.4 MeV of excitation and contained 31 peaks and 42 free parameters. Note, particularly, the narrow doublet at 5.70 and 5.73 MeV.

from elastically scattered electrons. Contaminant peaks in the ^{9}Be^{17}O spectrum were then included by varying a single normalization factor for each of the isotopes, ^{9}Be, ^{16}O, and ^{18}O.

For each fitted spectrum, three peaks of known excitation energy[1] were used to calibrate the energy scale. Known excitation energies and total widths of most ^{17}O levels were held fixed during the fitting procedure. Hence, most of the varied parameters were peak areas. An example of the quality of fit that was possible for a complex spectrum is illustrated in Fig. 2, which shows a ^{9}Be^{17}O spectrum measured at 90° for an incident electron energy of 268.8 MeV. A total of 73 peaks (48 for ^{17}O plus 25 background peaks) were included in the fit, although only 78 parameters were varied. Peaks for electrons scattered elastically from ^{16}O, ^{17}O, and ^{18}O are well resolved. In cases when two peaks were not resolved (separated by less than about 20 keV), they were fitted as a single peak. Examples of such unresolved doublets are the $\frac{5}{2}^+,\frac{5}{2}^-$ pair at 7.38 MeV, the $\frac{1}{2}^-,\frac{9}{2}^-$ pair at 9.15 MeV, the $\frac{7}{2}^-$ at 9.18 MeV and the $\frac{5}{2}^+$ at 9.19 MeV, and the $(\frac{5}{2}^-)$ at 9.86 MeV and the $(\frac{1}{2}^-)$ at 9.88 MeV (parentheses indicate uncertain J^π). Some doublets could be separated by careful line-shape analysis when prior knowledge of the total widths and excitation energies was available for both peaks. One such doublet is the pair of states at 5.70 and 5.73 MeV. Our ability to separate this doublet is shown in Fig. 3 with a ^{9}Be^{17}O spectrum measured at 90° for an incident energy of 174.8 MeV. The peak observed at the location of the doublet is broader than the experimental resolu-

tion. Another example is the doublet of states at 8.47 and 8.50 MeV. The 8.50-MeV level appeared in our spectra as a weak shoulder on the more strongly excited 8.47-MeV level.

Except for the strongly excited states in ^{17}O with relatively narrow widths, meaningful cross sections were very difficult to extract above 9.5 MeV due to the high level density. At lower excitation energies (E_x), cross sections could be extracted for almost all levels, although it was generally more difficult to extract cross sections for the broader states. For the single-particle $\frac{3}{2}^+$ state at 5.09 MeV ($\Gamma=96\pm5$ keV), measurements were hindered by its location between the strong $(\frac{9}{2}^-)$ state in ^{17}O at 5.22 MeV and the strong 3^- contaminant peak in ^{18}O at 5.10 MeV. Measurements for the $\frac{1}{2}^+$ state in ^{17}O at 6.36 MeV ($\Gamma=124\pm12$ keV) were likewise hindered by its proximity to the strong 3^- contaminant peak in ^{16}O at 6.13 MeV.

It was possible to determine absolute elastic cross sections from the fitted spectra with typical total uncertainties of $\pm10\%$ or less. Statistical uncertainties were often much smaller. To reduce normalization uncertainties caused by small fluctuations in the target thickness, beam-current monitoring, etc., the ^{17}O cross sections were renormalized to the elastic cross sections for ^{16}O and ^{18}O, which were generated with an MIT phase-shift code,[10,12] and to ^{9}Be cross sections measured with the ^{9}Be and ^{9}Be^{16}O targets. The total uncertainties in the renormalized cross sections were estimated by combining in quadrature the normalization uncertainties with the statistical fitting uncertainties.

B. Multipole analysis of form factors

Form factors were calculated from the measured cross sections $d\sigma/d\Omega$ by the expression,

$$|F|^2 = (\sigma_{\text{Mott}}\eta)^{-1}\frac{d\sigma}{d\Omega} , \tag{1}$$

where

$$\sigma_{\text{Mott}} = (Z\alpha/2E_0)^2(\cos^2\theta/2)/(\sin^4\theta/2) \tag{2}$$

is the Mott cross section for scattering electrons from an infinitely massive nucleus with charge Z and

$$\eta = [1 + (2E_0/M)\sin^2\theta/2]^{-1} \tag{3}$$

is the recoil factor that corrects for the finiteness of the nuclear mass M. Here, α is the fine-structure constant, E_0 is the incident electron energy, and θ is the scattering angle. Since $Z\alpha \ll 1$, the plane-wave Born approximation (PWBA) may be used to express $|F|^2$ as[19]

$$|F|^2 = \frac{q_\mu^4}{q^4}|F_L(q)|^2 + \left[\frac{-q_\mu^2}{2q^2} + \tan^2\theta/2\right]|F_T(q)|^2 , \tag{4}$$

where F_L is the longitudinal electric (or Coulomb) form factor, F_T is the transverse form factor, q is the momentum transfer, and $-q_\mu^2/q^2 = 1 - \omega^2/q^2 \simeq 1$, where ω is the energy loss of the scattered electron.

The longitudinal and transverse form factors can be decomposed into contributions from different multipoles:

$$|F_L(q)|^2 = \sum_{J\geq0}|F_{CJ}(q)|^2 ,$$

$$|F_T(q)|^2 = \sum_{J\geq1}[|F_{EJ}(q)|^2 + |F_{MJ}(q)|^2] , \tag{5}$$

where F_{CJ}, F_{EJ}, and F_{MJ} are form factors for Coulomb, transverse electric, and transverse magnetic transitions of multipolarity J. The allowed values of J in Eq. (3) are restricted by $|J_i - J_f| \leq J \leq J_i + J_f$, where $J_i = \frac{5}{2}$ is the spin of the ^{17}O ground state and J_f is the spin of the excited state. These values are restricted further by electromagnetic selection rules, which require the change in parity to be $(-1)^J$ for electric (CJ, EJ) transitions and $(-1)^{J+1}$ for magnetic (MJ) transitions. If no nucleons lie in orbitals higher than the s-d shell, then the highest multipoles that may contribute are $C3$ and $M4$ for negative-parity states and $C4$ and $M5$ for positive-parity states.

Small distortion effects arising from the attractive Coulomb field of the target nucleus can be accounted for approximately in the PWBA by expressing the measured form factors as functions of an effective momentum transfer q_{eff} rather than q. We calculated q_{eff} from the expression,

$$q_{\text{eff}} = q[1 - V_C(r)/E_0] , \tag{6}$$

where $V_C(r)$ represents the field of the nucleus at distance r. We set $r = (L+1)/q$, where L is the minimum orbital angular-momentum transfer for the transition.

$V_C(r)$ was approximated by the field of a uniformly charged sphere with radius $R = \sqrt{5/3}r_{\text{rms}}$, where $r_{\text{rms}} = 1.20A^{1/3}$ fm.

The longitudinal and transverse form factors can be written in terms of reduced matrix elements of the electromagnetic transition operators:[20]

$$F_{CJ}(q) = \frac{\sqrt{4\pi}}{Z}\frac{q^J}{(2J+1)!!}\frac{(J_f\|M_J(q)\|J_i)}{(2J_i+1)^{1/2}} ,$$

$$F_{EJ}(q) = \frac{\sqrt{4\pi}}{Z}\frac{q^J}{(2J+1)!!}\left[\frac{J+1}{J}\right]^{1/2}\frac{(J_f\|T_J^{\text{el}}(q)\|J_i)}{(2J_i+1)^{1/2}} , \tag{7}$$

$$F_{MJ}(q) = \frac{\sqrt{4\pi}}{Z}\frac{q^J}{(2J+1)!!}\left[\frac{J+1}{J}\right]^{1/2}\frac{(J_f\|T_J^{\text{mag}}(q)\|J_i)}{(2J_i+1)^{1/2}} .$$

Reduced transition probabilities are obtained by extrapolating the matrix elements to the photon point, $q = \omega$:

$$B(CJ\uparrow) = \lim_{q\to\omega}\frac{|(J_f\|M_J(q)\|J_i)|^2}{2J_i+1} ,$$

$$B(EJ\uparrow) = \lim_{q\to\omega}\frac{|(J_f\|T_J^{\text{el}}(q)\|J_i)|^2}{2J_i+1} , \tag{8}$$

$$B(MJ\uparrow) = \lim_{q\to\omega}\frac{|(J_f\|T_J^{\text{mag}}(q)\|J_i)|^2}{2J_i+1} .$$

Since the data discussed herein lie far above the photon point ($q \gtrsim 1$ fm^{-1}), we performed the extrapolation to the photon point within the context of a model in which the reduced matrix elements were parametrized by polynomial-times-Gaussian forms, as suggested by the use of harmonic-oscillator wave functions:

$$(J_f\|M_J(q)\|J_i) = (2J_i+1)^{1/2}f_{\text{c.m.}}(q)f_N(q)e^{-y}\sum_m a_m y^m ,$$

$$(J_f\|T_J^{\text{el}}(q)\|J_i) = (2J_i+1)^{1/2}f_{\text{c.m.}}(q)f_N(q)(\omega/q)$$
$$\times e^{-y}\sum_m b_m y^m , \tag{9}$$

$$(J_f\|T_J^{\text{mag}}(q)\|J_i) = (2J_i+1)^{1/2}f_{\text{c.m.}}(q)f_N(q)e^{-y}\sum_m c_m y^m .$$

Here, $y = (bq/2)^2$, b is the oscillator parameter, $f_N(q) = (1+q^2/\Lambda^2)^{-2}$ is the single-nucleon form factor that corrects for the finite size of the nucleon, and $f_{\text{c.m.}}(q) = e^{y/A}$ is the center-of-mass form factor that corrects for the lack of translational invariance in shell-model wave functions. The size parameter, $\Lambda = 4.33$ fm^{-1}, is determined by fitting data for the proton form factor and corresponds to a proton charge radius of 0.80 fm. The polynomial coefficients a_m, b_m, and c_m can be determined either theoretically from nuclear-structure calculations (see, for example, the recent shell-model description of ^{19}F electron-scattering data by Brown *et al.*[21]) or empirically by fitting the measured form factors. Coefficients for selected single-particle transitions have been tabulated by Donnelly and Haxton.[22]

Total form-factor measurements at 90°, 140°, and 160° were fitted simultaneously with the parametrizations

given in Eqs. (7) and (9). Experimental values for the longitudinal form factor were deduced by subtracting calculated values of the transverse form factor from measurements of the total form factor at 90°. Similarly, experimental values for the transverse form factor were deduced by subtracting calculated values of the longitudinal form factor from measurements of the total form factor at 140° and 160°. Uncertainties in the fitted form factors were propagated into the uncertainties in the subtracted quantities. Specific details of the fits will be presented in Sec. V. In most cases, we assumed transitions to orbitals higher than the s-d shell can be neglected. This assumption restricts the polynomials in Eq. (9) to be, at most, quadratic in y. In particular, it implies that F_{M1}, F_{E1}, and F_{E2} each require three nonzero expansion coefficients, F_{C0}, F_{C1}, F_{C2}, F_{M2}, F_{M3}, F_{E3}, and F_{E4} each require two, and F_{C3} and F_{C4} each require one. Not all of these coefficients are independent, however, since local charge conservation requires[19]

$$\lim_{q \to 0} \{ [J/(J+1)]^{1/2} F_{EJ}(q) - (\omega/q) F_{CJ}(q) \} = 0 , \qquad (10)$$

and hence, from Eqs. (7) and (9), $a_0 = b_0$.

IV. THE WEAK-COUPLING MODEL

The particle-hole structure of states in many nuclei can be understood in terms of the well-known weak-coupling model for particles and holes. In this model, it is assumed that the interaction between particles in the same shell is stronger than between particles in different shells and that the interaction between particles and holes can be treated as a perturbation. This model's conceptual simplicity is part of the reason for its appeal. The mass of a state with m particles and n holes (relative to a $T = 0$ core state M_c) and with isospin T is given by the Bansal-French-Zamick formula,[23,24]

$$M^* = M_p + M_h - M_c + Amn + B \langle \mathbf{T}_p \cdot \mathbf{T}_h \rangle , \qquad (11)$$

where

$$\langle \mathbf{T}_p \cdot \mathbf{T}_h \rangle = \tfrac{1}{2} [T(T+1) - T_p(T_p+1) - T_h(T_h+1)] . \qquad (12)$$

Here, M_p (M_h) denotes the mass of the nucleus with m (0) particles, 0 (n) holes, and isospin T_p (T_h); A is the average particle-hole interaction energy and B measures the strength of the isospin interaction. Possible spin-dependent interactions and the small Coulomb interaction between protons and proton holes have been neglected. We denote the weak-coupling structure of the particle-hole state with spin J by $M^*(J) = [M_p(J_p) \otimes M_h(J_h)]_J$, where $M_p(J_p)$ and $M_h(J_h)$ refer to yrast levels with spins J_p and J_h, respectively. For example, the first 2^+ state in ^{16}O is dominated by the weak-coupling structure ^{20}Ne(2^+)$\otimes$^{12}C(0^+), where ^{20}Ne(2^+) refers to the first 2^+ state in ^{20}Ne and ^{12}C(0^+) refers to the ^{12}C ground state.

The appropriate core state for describing the oxygen isotopes is ^{16}O. Our discussion will concentrate mainly on configurations with $T = T_{max}$, where $T_{max} = T_p + T_h$.

The restriction to "isospin-stretched" configurations is motivated by a weak-coupling calculation[25] for potassium and scandium isotopes that suggests that the weak-coupling prescription may be inadequate for calculating states with $T < T_{max}$. Our calculations used binding energies from the tables of Wapstra and Bos.[26] As examples, the excitation energy (in MeV) of the first predominantly 4p-4h state in ^{16}O with $T = 0$ is predicted to be $2.43 + 16A$, whereas the excitation energy of the first predominantly 2p-2h level in ^{16}O with $T = 2$ is predicted to be $16.79 + 4A + B$.

A. Application to ^{16}O

In Table I we compare experimental and calculated excitation energies for several states in ^{16}O. We determined $A = 0.23$ MeV and $B = 5.02$ MeV by reproducing approximately the experimental excitation energies of the first $T = 0$ and 2 excited states in ^{16}O at 6.05 and 22.72 MeV, respectively. Wave functions for the $T = 0$ negative-parity states, which have $T < T_{max}$, are expected to be admixtures of the 1p-1h and 3p-3h weak-coupling configurations. We note, however, that the pure 1p-1h configurations are calculated to lie lower in energy than the pure 3p-3h configurations.

The interpretation of the positive-parity levels given in Table I was suggested originally by Arima, Horiuchi, and Sebe.[27] In agreement with a variety of other calculations,[28–31] the low-lying positive-parity states are described mainly by 4p-4h configurations. One particularly interesting and successful prediction of the weak-coupling model is that electroexcitation of the second 2^+ state at 9.85 MeV should be dominated by transitions within the p shell. Indeed, the measured form factor for this state, unlike that of other 2^+ states in ^{16}O, looks very similar to that of the first 2^+ state in ^{12}C at 4.44 MeV.[10,32]

TABLE I. Comparison of calculated and experimental excitation energies for selected states in ^{16}O. The experimental values are taken from Ref. 1.

J^π	T	Configuration	Calc. (MeV)	Expt. (MeV)
0^+	0	^{20}Ne(0^+)$\otimes$^{12}C(0^+)	6.11	6.05
2^+	0	^{20}Ne(2^+)$\otimes$^{12}C(0^+)	7.74	6.92
4^+	0	^{20}Ne(4^+)$\otimes$^{12}C(0^+)	10.36	10.36
2^+	0	^{20}Ne(0^+)$\otimes$^{12}C(2^+)	10.55	9.85
2^-	1	$[^{17}$F($\frac{5}{2}^+$)$\otimes$^{15}N($\frac{1}{2}^-$)	13.01	12.97
3^-	1	$+^{17}$O($\frac{5}{2}^+$)$\otimes$^{15}O($\frac{1}{2}^-$)$]/\sqrt{2}$	13.01	13.26
0^-	1	$[^{17}$F($\frac{1}{2}^+$)$\otimes$^{15}N($\frac{1}{2}^-$)	13.61	12.80
1^-	1	$+^{17}$O($\frac{1}{2}^+$)$\otimes$^{15}O($\frac{1}{2}^-$)$]/\sqrt{2}$	13.61	13.09
0^+	2	$[^{18}$Ne(0^+)$\otimes$^{14}C(0^+) $+2^{18}F^*(0^+)\otimes$^{14}N*(0^+) $+^{18}$O(0^+)$\otimes$^{14}O(0^+)$]/\sqrt{6}$	22.73	22.72
2^+	2	$[^{18}$Ne(2^+)$\otimes$^{14}C(0^+) $+2^{18}F^*(2^+)\otimes$^{14}N*(0^+) $+^{18}$O(2^+)$\otimes$^{14}O(0^+)$]/\sqrt{6}$	24.72	24.52

B. Positive-parity levels in ^{17}O

We now apply these ideas to ^{17}O. The first three positive-parity states in ^{17}O are described in lowest approximation by the predominantly single-particle weak-coupling configurations,

$$\tfrac{5}{2}^+(0.00 \text{ MeV}) = 1d_{5/2} \otimes {}^{16}\text{O}(0^+) ,$$

$$\tfrac{1}{2}^+(0.87 \text{ MeV}) = 2s_{1/2} \otimes {}^{16}\text{O}(0^+) , \qquad (13)$$

$$\tfrac{3}{2}^+(5.09 \text{ MeV}) = 1d_{3/2} \otimes {}^{16}\text{O}(0^+) ,$$

where ^{16}O(0^+) refers to the predominantly 0p-0h ground state of ^{16}O. Positive-parity states at higher excitation energies must be mainly collective in nature. Our calculations for ^{17}O used the same values of A and B as were used for ^{16}O, except for the $T = \tfrac{1}{2}$ positive-parity states, which used $A = 0.30$ MeV. The first collective positive-parity state is expected to be a predominantly 5p-4h level with $J^\pi = \tfrac{3}{2}^+$. We identify this level as the known $\tfrac{3}{2}^+$ state at 5.87 MeV. Wave functions for the physical $\tfrac{3}{2}^+$ states at 5.08 and 5.87 MeV probably contain significant 1p-0h and 5p-4h components since the states are nearly degenerate in energy; thus, the $1d_{3/2}$ orbital is probably important for describing the wave functions of both states.

The first $T = \tfrac{3}{2}$ state with positive parity has a calculated excitation energy of 13.49 MeV. It is expected to be a mainly 3p-2h state with $J^\pi = \tfrac{1}{2}^+$. We identify this state as the known $\tfrac{1}{2}^+$ level at 12.94 MeV. The first $T = \tfrac{5}{2}$ state is expected at about 26.0 MeV; it should be a predominantly 3p-2h state with $J^\pi = \tfrac{5}{2}^+$ or $\tfrac{1}{2}^+$. As yet, no experimental candidates for $T = \tfrac{5}{2}$ states in ^{17}O have

been observed.

In Table II we present a comparison of experimental and calculated excitation energies for selected positive-parity states in ^{17}O. The $T = \tfrac{1}{2}$ states at 5.87, 6.86, 7.58, and 8.47 MeV are candidates for members of a predominantly 5p-4h rotational band that has the weak-coupling structure $[^{21}\text{Ne}(J^\pi) \otimes {}^{12}\text{C}(0^+)]_{J\pi}$. Here, ^{21}Ne$(J^\pi)$ refers to the $\tfrac{3}{2}^+$(g.s.), $\tfrac{5}{2}^+$(0.35 MeV), $\tfrac{7}{2}^+$(1.75 MeV), and $\tfrac{9}{2}^+$(2.87 MeV) members of the ground-state $K^\pi = \tfrac{3}{2}^+$ band in ^{21}Ne. All four levels in ^{17}O have narrow widths and are strongly excited by electric quadrupole transitions. Similarly, the $T = \tfrac{3}{2}$ states at 12.94, 13.64, 15.20, and 16.24 MeV are candidates for the $\tfrac{1}{2}^+$, $\tfrac{5}{2}^+$, $\tfrac{3}{2}^+$, and $\tfrac{9}{2}^+$ members of a predominantly 3p-2h rotational band, analogous to the ground-state $K^\pi = \tfrac{1}{2}^+$ band in ^{19}F. None of these four $T = \tfrac{3}{2}$ states are excited very strongly by electron scattering. Two broad $T = \tfrac{1}{2}$ states (not included in Table II), a $\tfrac{1}{2}^+$ state at 6.36 MeV ($\Gamma = 124 \pm 12$ keV) and a $\tfrac{3}{2}^+$ state at 7.20 MeV ($\Gamma = 280 \pm 30$ keV), possibly can be described by the predominantly 3p-2h configuration $[^{19}\text{F}(\tfrac{1}{2}^+) \otimes {}^{14}\text{N}(1^+)]_{J\pi}$, where $J^\pi = \tfrac{1}{2}^+$ or $\tfrac{3}{2}^+$.

C. Negative-parity levels in ^{17}O

Table III presents a comparison of the experimental and calculated excitation energies for selected negative-parity levels in ^{17}O. Calculations indicate that several predominantly 4p-3h and 2p-1h weak-coupling configurations with $T = \tfrac{1}{2}$ lie low in energy; hence, the physical $T = \tfrac{1}{2}$ states are expected to be admixtures of both 4p-3h and 2p-1h configurations. Weak-coup-

TABLE II. Comparison of calculated and experimental excitation energies for selected positive-parity states in ^{17}O. The experimental values are taken from Ref. 1.

J^π	T	Configuration	Calc.[a] (MeV)	Expt. (MeV)
$\tfrac{3}{2}^+$	$\tfrac{1}{2}$	^{21}Ne$(\tfrac{3}{2}^+) \otimes {}^{12}C(0^+)$	5.81	5.87
$\tfrac{5}{2}^+$	$\tfrac{1}{2}$	^{21}Ne$(\tfrac{5}{2}^+) \otimes {}^{12}C(0^+)$	6.16	6.86
$\tfrac{7}{2}^+$	$\tfrac{1}{2}$	^{21}Ne$(\tfrac{7}{2}^+) \otimes {}^{12}C(0^+)$	7.56	7.58
$\tfrac{9}{2}^+$	$\tfrac{1}{2}$	^{21}Ne$(\tfrac{9}{2}^+) \otimes {}^{12}C(0^+)$	8.68	8.47
$\tfrac{1}{2}^+$	$\tfrac{3}{2}$	$[\sqrt{2/3}\,{}^{19}$F$(\tfrac{1}{2}^+) \otimes {}^{14}$N*$(0^+)$ $+\sqrt{1/3}\,{}^{19}$Ne$(\tfrac{1}{2}^+) \otimes {}^{14}C(0^+)$	13.49	12.94
$\tfrac{5}{2}^+$	$\tfrac{3}{2}$	$[\sqrt{2/3}\,{}^{19}$F$(\tfrac{5}{2}^+) \otimes {}^{14}$N*$(0^+)$ $+\sqrt{1/3}\,{}^{19}$Ne$(\tfrac{5}{2}^+) \otimes {}^{14}C(0^+)$	13.70	13.64
$\tfrac{3}{2}^+$	$\tfrac{3}{2}$	$[\sqrt{2/3}\,{}^{19}$F$(\tfrac{3}{2}^+) \otimes {}^{14}$N*$(0^+)$ $+\sqrt{1/3}\,{}^{19}$Ne$(\tfrac{3}{2}^+) \otimes {}^{14}C(0^+)$	15.04	15.20
$\tfrac{9}{2}^+$	$\tfrac{3}{2}$	$[\sqrt{2/3}\,{}^{19}$F$(\tfrac{9}{2}^+) \otimes {}^{14}$N*$(0^+)$ $+\sqrt{1/3}\,{}^{19}$Ne$(\tfrac{9}{2}^+) \otimes {}^{14}C(0^+)$	16.27	16.24

[a]Calculations for the $T = \tfrac{1}{2}$ states used the value $A = 0.30$ MeV (see text).

TABLE III. Comparison of calculated and experimental excitation energies for selected negative-parity states in ^{17}O. The experimental values are taken from Ref. 1.

J^π	T	Configuration	Calc. (MeV)	Expt. (MeV)
$\tfrac{1}{2}^-$	$\tfrac{1}{2}$	^{20}Ne$(0^+) \otimes {}^{13}$C$(\tfrac{1}{2}^-)$	4.39	3.06
$\tfrac{5}{2}^-$	$\tfrac{1}{2}$	^{20}Ne$(2^+) \otimes {}^{13}$C$(\tfrac{1}{2}^-)$	6.02	3.84
$\tfrac{3}{2}^-$	$\tfrac{1}{2}$	^{20}Ne$(2^+) \otimes {}^{13}$C$(\tfrac{1}{2}^-)$	6.02	4.55
$\tfrac{3}{2}^-$	$\tfrac{1}{2}$	^{18}F$(1^+) \otimes {}^{15}$N$(\tfrac{1}{2}^-)$	6.98	5.38
$\tfrac{1}{2}^-$	$\tfrac{1}{2}$	^{18}F$(1^+) \otimes {}^{15}$N$(\tfrac{1}{2}^-)$	6.98	5.94
$\tfrac{7}{2}^-$	$\tfrac{1}{2}$	^{18}F$(3^+) \otimes {}^{15}$N$(\tfrac{1}{2}^-)$	7.92	5.70
$\tfrac{11}{2}^-$	$\tfrac{1}{2}$	^{18}F$(5^+) \otimes {}^{15}$N$(\tfrac{1}{2}^-)$	8.10	7.76
$\tfrac{9}{2}^-$	$\tfrac{1}{2}$	^{18}F$(5^+) \otimes {}^{15}$N$(\tfrac{1}{2}^-)$	8.10	9.15
$\tfrac{1}{2}^-$	$\tfrac{3}{2}$	$[\sqrt{2/3}\,{}^{18}$F*$(0^+) \otimes {}^{15}$N$(\tfrac{1}{2}^-)$ $+\sqrt{1/3}\,{}^{18}$O$(0^+) \otimes {}^{15}$O$(\tfrac{1}{2}^-)$	10.55	11.08
$\tfrac{3}{2}^-$	$\tfrac{3}{2}$	$[\sqrt{2/3}\,{}^{18}$F*$(2^+) \otimes {}^{15}$N$(\tfrac{1}{2}^-)$	12.56	12.47
$\tfrac{5}{2}^-$	$\tfrac{3}{2}$	$+\sqrt{1/3}\,{}^{18}$O$(2^+) \otimes {}^{15}$O$(\tfrac{1}{2}^-)]$	12.56	13.00
$\tfrac{7}{2}^-$	$\tfrac{3}{2}$	$[\sqrt{2/3}\,{}^{18}$F*$(4^+) \otimes {}^{15}$N$(\tfrac{1}{2}^-)$	14.14	14.23
$\tfrac{9}{2}^-$	$\tfrac{3}{2}$	$+\sqrt{1/3}\,{}^{18}$O$(4^+) \otimes {}^{15}$O$(\tfrac{1}{2}^-)]$	14.14	14.72[a]

[a]This work.

ling configurations of the types ^{20}Ne$(J^\pi)\otimes ^{13}$C$(\frac{1}{2}^-)$, ^{20}Ne$(J^\pi)\otimes ^{13}$C$(\frac{3}{2}^-)$ $(J^\pi=0^+,2^+,4^+)$ and ^{18}F(J^π) $\otimes ^{15}$N$(\frac{1}{2}^-)$ $(J^\pi=1^+,3^+,5^+)$ give rise to the negative-parity spectrum: $(\frac{1}{2}^-)^3$, $(\frac{3}{2}^-)^4$, $(\frac{5}{2}^-)^4$, $(\frac{7}{2}^-)^4$, $(\frac{9}{2}^-)^3$, $(\frac{11}{2}^-)^2$, where the superscripts indicate the number of states that have the specified J^π. This calculated spectrum agrees well with the levels observed experimentally below about 9 MeV. Our calculated energy of 8.10 MeV for the first $\frac{11}{2}^-$ level agrees well with the experimental energy of 7.76 MeV. States with $J^\pi=\frac{5}{2}^-$, $\frac{7}{2}^-$, $\frac{9}{2}^-$, and $\frac{11}{2}^-$ and with the dominant configurations ^{20}Ne$(4^+)\otimes ^{13}$C$(\frac{3}{2}^-)$ are predicted at about 12.32 MeV. One of these states may correspond to a new narrow level ($\Gamma \leq 20$ keV) that we observe in our spectra at 12.22 ± 0.02 MeV. The fact that the calculated excitation energies of many $T=\frac{1}{2}$ negative-parity states are too high probably stems from our neglect of mixing of the 4p-3h and 2p-1h weak-coupling configurations.

For $T=\frac{3}{2}$ negative-parity states below about 16 MeV, our calculations indicate that only predominantly 2p-1h weak-coupling configurations are important. Thus, the low-lying $T=\frac{3}{2}$ negative-parity levels are expected to be described better by the simple weak-coupling model than the low-lying $T=\frac{1}{2}$ negative-parity levels. Indeed, Table III shows that calculated and experimental excitation energies agree better for these levels. The level we observe at 14.72 ± 0.02 MeV with $\Gamma=35\pm11$ keV corresponds to the first predicted $\frac{9}{2}^-$ level with $T=\frac{3}{2}$. This state was reported first as a narrow level at 14.75 MeV in the low-momentum-transfer electron-scattering experiment of Rangacharyulu et al.[7] A fitted spectrum from the present experiment, which shows the $\frac{7}{2}^-$ level at 14.23 MeV and the $\frac{9}{2}^-$ level at 14.72 MeV, is shown in Fig. 2 of Ref. 8.

We have observed that many features of the spectrum of ^{17}O can be described by the weak-coupling model. Our discussion focused on isospin-stretched configurations, since other configurations are thought to provide a poorer description of most physical states. Finally, we note that various shell-model calculations, which are discussed below, give similar structures for many of the states discussed here. Ideally, shell-model descriptions of these levels should consider multiparticle-multihole configurations and include the full p and s-d shells in the active model space.

V. RESULTS

A. Single-particle levels

The predominantly single-particle levels in ^{17}O include the $\frac{5}{2}^+$ ground state, the first $\frac{1}{2}^+$ level at 0.87 MeV, and the first $\frac{3}{2}^+$ level at 5.09 MeV. These states, which are discussed in the preceding section, have wave functions that can be described in lowest approximation as a single valence neutron coupled to an ^{16}O core. Separated longitudinal and transverse form factors are shown in Figs. 4(a) and 4(b) for the 0.87-MeV level and in Figs. 4(c) and 4(d) for the 5.09-MeV level. The curves that pass through the form factors in these figures were obtained by phenomenological fits as described in Sec. III. Both states were fitted simultaneously using the same value of the oscillator constant, $b=1.779\pm0.018$ fm. The observation of large Coulomb transitions for both levels indicates that protons from the ^{16}O core participate in the transitions.

1. The 0.87-MeV level

Only the C2 multipole contributes to the longitudinal form factor for the 0.87-MeV level. As Fig. 4(a) shows, its shape is well determined by the present measurements up to the region of the second maximum. Both E2 and M3 multipoles can contribute to the transverse form factor, which is shown in Fig. 4(b). The curve shown in Fig. 4(b) shows the results of our best fit, which essentially assumed dominance by the M3 component (see discussion below). For this level, we determined $B(E2\uparrow)=2.18\pm0.16$ e^2fm^4, which implies a mean lifetime $\tau_m=249\pm18$ ps, in good agreement with the tabulated average[1] of 258.6 ± 2.6 ps.

2. The 5.09-MeV level

The 5.09-MeV level with $J^\pi=\frac{3}{2}^+$ is somewhat more complicated to describe empirically than the 0.87-MeV level, since additional multipoles can contribute. Our analysis was complicated further because measurements were confined to a more limited range of momentum transfer (see Sec. III). Curves for both the C2 and C4 components of the longitudinal form factor are shown in Fig. 4(c). The shape of the C2 component was assumed to be the same as for the 0.87-MeV level. Our measurements of the transverse form factor are shown in Fig. 4(d). Curves are not shown for its multipole components, since there were insufficient measurements to determine contributions from individual multipoles unambiguously. The reduced transition probabilities determined for this level were $B(E2\uparrow)=2.05\pm0.20$ e^2fm^4 and $B(E4\uparrow)=191\pm34$ e^2fm^8.

3. Discussion

The percentage of single-particle (1p-0h) component in the $\frac{1}{2}^+$ and $\frac{3}{2}^+$ levels of ^{17}O has been calculated by several authors. Using somewhat similar models, Brown and Green[28] (BG) and Birkholz and Beck[33] (BB) obtain 78% and 65%, respectively, for the 1p-0h component in the first $\frac{1}{2}^+$ level. Lower percentages of 42% and 61%, respectively, result from the calculations of Zuker, Buck, and McGrory[29] (ZBM) and Reehal and Wildenthal[31] (RW). The calculations of ZBM and RW are very similar to each other but are rather different than those of BG and BB. Details of these models are reviewed in Sec. V B 4.

The $1d_{3/2}$ orbital is not active in the models of ZBM and RW, so their calculations do not predict a predominantly single-particle $\frac{3}{2}^+$ state. The models of BG and
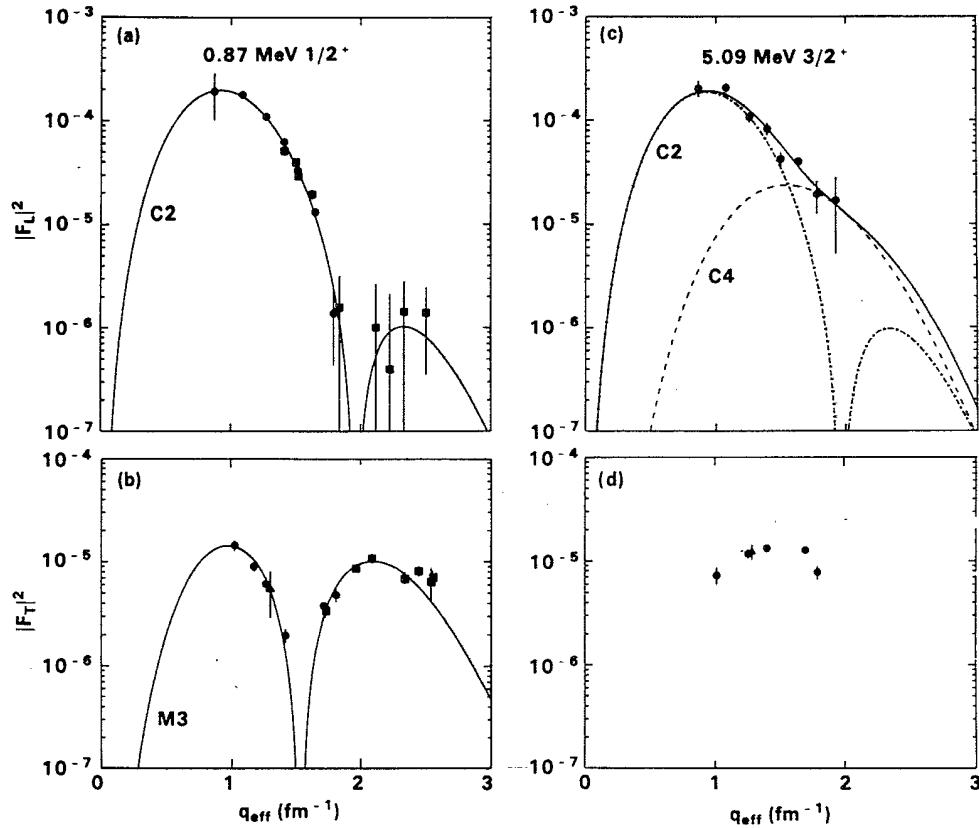
FIG. 4. The (a) longitudinal and (b) transverse form factors for the $\frac{1}{2}^+$ single-particle state in ^{17}O at 0.87 MeV, and the (c) longitudinal and (d) transverse form factors for the $\frac{3}{2}^+$ single-particle state in ^{17}O at 5.09 MeV. Solid circles indicate measurements from the present line-shape analysis at 90° and 160°, solid triangles indicate measurements from the present line-shape analysis at 140°, and solid squares indicate unpublished measurements from an earlier line-shape analysis (see text).

BB, however, do not have this limitation. Their calculations give 52% and 59%, respectively, for the 1p-0h component in the first $\frac{3}{2}^+$ level. Thus, the $\frac{3}{2}^+$ level at 5.09 MeV is expected to have less pure single-particle character than the $\frac{1}{2}^+$ level at 0.87 MeV. This conclusion is supported by the experimental analysis of Kim *et al.*,[5] in which low-q electron-scattering measurements of the Coulomb form factors were fitted in the single-particle model by introducing a variable effective neutron charge (e_n). These authors determined $e_n = (0.62 \pm 0.09) |e|$ for the 0.87-MeV level and $e_n = (0.91 \pm 0.13) |e|$ for the 5.09-MeV level.

In Figs. 5(a) and 5(b), respectively, we compare our measurements of the transverse form factors for the 0.87- and 5.09-MeV levels with the predictions of the single-particle model. The curves were calculated using harmonic-oscillator wave functions with an oscillator parameter of 1.80 fm. For both states, the single-particle predictions overestimate the measured transverse form factors. This result is further evidence for collective components in their wave functions. Clearly, the overall agreement is much better for the $\frac{1}{2}^+$ level. Its transverse form factor is predicted to be dominated by the $M3$ component; the predicted $E2$ component is probably less reliable, since $E2$ transitions may occur from single-particle and collective components in its wave function.

The predicted shape of the transverse form factor for the 0.87-MeV level is in reasonable agreement with our measurements, although the relative heights of the two maxima are not well reproduced. The single-particle model overpredicts the form factor for the $\frac{3}{2}^+$ level by an order of magnitude. Thus, the 5.09-MeV level is poorly described as a single-particle level.

B. Collective positive-parity levels

The known collective positive-parity levels in ^{17}O below 9.5 MeV are listed in Table IV. Peaks were observed clearly in the measured spectra for the narrow levels ($\Gamma < 10$ keV) at 5.87, 6.86, 7.38, 7.58, 8.40, 8.47, and 9.19 MeV. Peaks for the broader states ($\Gamma > 10$ keV) were rather inconspicuous. Their concealment was due, in part, to the relatively high density of narrow levels and the complexity of the ^9Be background. Fits of the spectra included peaks for all levels listed in Table IV, regardless of whether or not they were obvious.

Form factors for the collective positive-parity states were unavailable from the early measurements discussed in Sec. II. Thus, measurements for these states are limited to momentum transfers between 0.8 and 1.9 fm^{-1}. The measured form factors for the narrow levels at 5.87, 6.86, 7.58, 8.40, and 8.47 MeV, unlike those for the
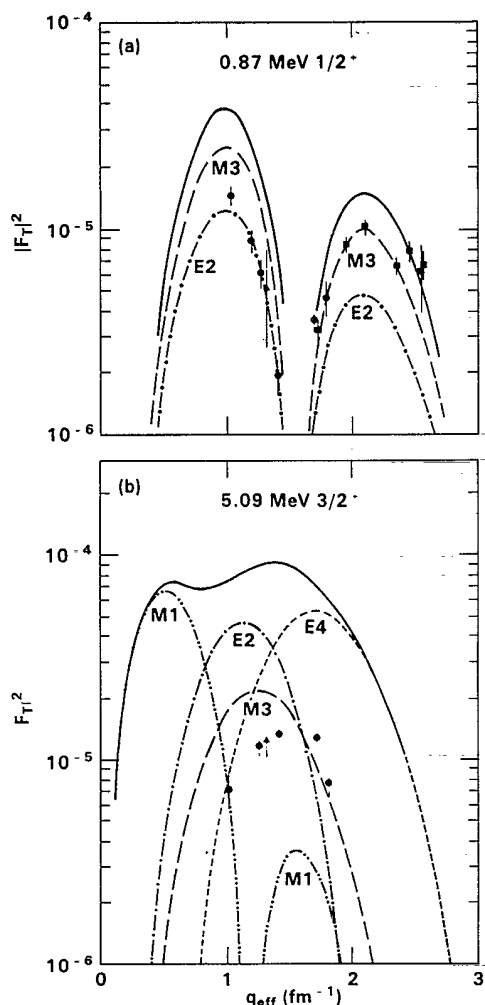
FIG. 5. Transverse form factors for the predominantly single-particle states at (a) 0.87 MeV and (b) 5.09 MeV compared with predictions of the single-particle shell model. The curves were calculated with harmonic-oscillator wave functions using the oscillator parameter $b = 1.80$ fm. See the caption to Fig. 4 for a description of the data points.

TABLE IV. Collective positive-parity states in ^{17}O below 9.50 MeV. All spins, parities, excitation energies, and widths ($\Gamma > 10$ keV) are from Ref. 1, except where otherwise noted. An asterisk marks levels for which peaks were observed clearly in the measured spectra.

E_x (MeV)	J^π	Γ (keV)	Comments
5.87*	$\frac{3}{2}^+$	< 10	
6.36	$\frac{1}{2}^+$	124±12	
6.86*	$\frac{5}{2}^+$	< 10	Listed as $(\frac{1}{2}^-)$ in Ref. 1
7.20	$\frac{3}{2}^+$	280±30	
7.38*	$\frac{5}{2}^+$	< 10	Member of unresolved doublet
7.58*	$\frac{7}{2}^+$	< 10	Listed in $\frac{7}{2}^-$ in Ref. 1
7.96	$\frac{1}{2}^+$	90±9	
8.07	$\frac{3}{2}^+$	85±9	Not observed in spectra
8.34	$\frac{1}{2}^+$	11.4±0.5	
8.40*	$\frac{5}{2}^+$	< 10	
8.47*	$\frac{9}{2}^+$	< 10	Listed in $\frac{7}{2}^+$ in Ref. 1
8.90	$\frac{3}{2}^+$	101±3	Not observed in spectra
9.19*	$\frac{5}{2}^+$	< 10	Member of unresolved doublet

single-particle states, are almost completely longitudinal. Form factors for the low-lying 0^+, 2^+, and 4^+ states in ^{16}O and ^{18}O also have negligible transverse components;[10,12] this fact is usually attributed to the collective natures of these states.

1. The levels at 5.87, 6.86, 7.58, 8.40, and 8.47 MeV

Figures 6(a)−6(e) show the extracted longitudinal form factors for the narrow levels in ^{17}O at 5.87, 6.86, 7.58, 8.40, and 8.47 MeV, respectively. Curves in the figures were obtained by fitting the form factors with contributions from $C0$ and $C2$ multipoles; $C4$ contributions were neglected. Monopole form factors for the collective $\frac{5}{2}^+$ levels in ^{17}O were described by a single shape, which was assumed to be similar to that for the 0^+ level in ^{16}O at 6.05 MeV. The $C2$ form factors for all collective positive-parity levels in ^{17}O also were described by a sin-

gle shape, which was determined by simultaneously fitting the five levels at 5.87, 6.86, 7.58, 8.40, and 8.47 MeV. The $E2$ form factor was small and poorly determined. The value of the oscillator parameter for describing these levels, $b = 1.856 \pm 0.052$ fm, is somewhat larger than that for describing the single-particle levels, although both values are consistent with $b \simeq 1.80$ fm.

The levels at 5.87 and 8.40 MeV are listed in Ref. 1 as $\frac{3}{2}^+$ and $\frac{5}{2}^+$ states, respectively. Since our measurements reveal these levels to be excited primarily by electric quadrupole transitions, we confirm their positive-parity assignments.

a. The 6.86-MeV level. The spin and parity of the level at 6.86 MeV were not established by previous works, although a tentative J^π assignment of $\frac{1}{2}^-$ was proposed from a study of the ^{15}N(^{3}He,p)^{17}O reaction.[34] The q dependence of the measured form factor for this level indicates that it is primarily an electric quadrupole excitation; thus, its parity must be positive and its spin must be between $\frac{1}{2}$ and $\frac{9}{2}$. Form-factor measurements for this level were fitted with a $C2$ contribution only (χ^2/datum=7.9) and with $C2+C0$ contributions (χ^2/datum=6.3). Thus, this level most likely has $J^\pi = \frac{5}{2}^+$ since its form factor seems to require a significant monopole component. This assignment is of interest because shell-model calculations predict a $\frac{5}{2}^+$ level near 6 or 7 MeV for which, previously, there had been no viable experimental candidate.

b. The 7.58-MeV level. The level at 7.58 MeV is listed in Ref. 1 as a $\frac{7}{2}^-$ state. Present form-factor measurements for this level determine its parity to be positive, however, since it is strongly excited by an electric quadrupole transition. The measured $B(E2\uparrow)$ value for this level is, in fact, larger than that of any other level except
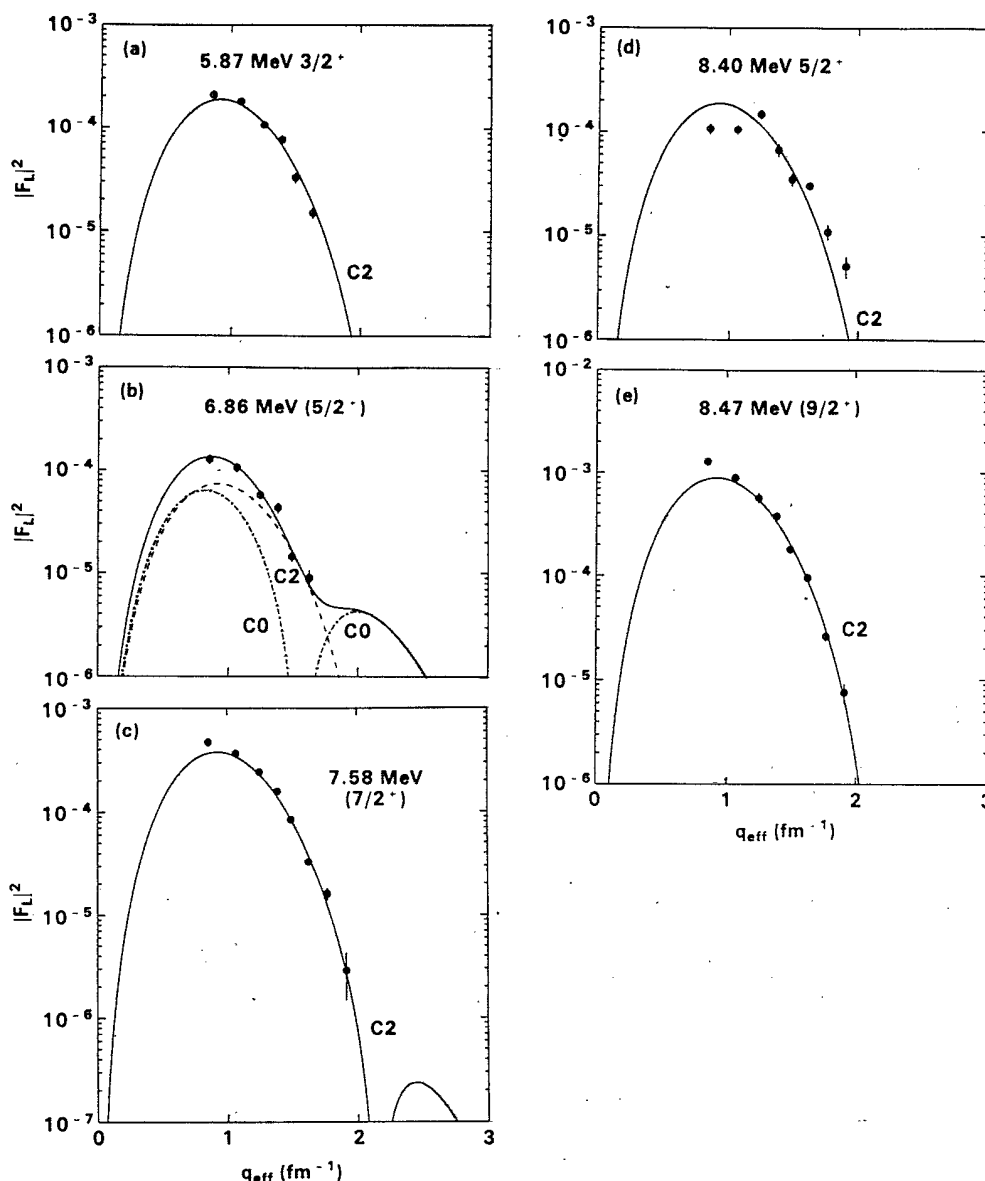
FIG. 6. Longitudinal form factors for (a) the $\frac{3}{2}^+$ state in ^{17}O at 5.87 MeV, (b) the $\frac{5}{2}^+$ state at 6.86 MeV, (c) the $\frac{7}{2}^+$ state at 7.58 MeV, (d) the $\frac{5}{2}^+$ state at 8.40 MeV, and (e) the $\frac{9}{2}^+$ state at 8.47 MeV. See the caption to Fig. 4 for a description of the data points.

the one at 8.47 MeV. The previous incorrect negative-parity assignment for this level can be traced to a 1970 paper by Bethge, Pullen, and Middleton.[35] These authors observed the 7.58-MeV level in measurements of the $^{13}C(^6Li,d)^{17}O$ and $^{13}C(^7Li,t)^{17}O$ reactions, but they did not determine its spin or parity. Table I of Ref. 35 lists this level as a $\frac{7}{2}^-$ state and indicates that this J^π assignment is from a paper by Lister and Sayres,[36] which reported a spectroscopic study of ^{17}O with the $^{16}O(n,n)^{16}O$ reaction. The 7.58-MeV level, which has a small neutron width (Ref. 37), was, in fact, not observed by Lister and Sayres. (Instead, they assigned a level at 7.69 MeV to have $J^\pi = \frac{7}{2}^-$.) Our establishment of positive parity for the 7.58-MeV level explains why the low-q form-factor measurements of Kim *et al.*[5] seemed to indicate an unusually large $C1$ component for this level,

when it was assumed to be a $\frac{7}{2}^-$ state.

The *spin* of the 7.58-MeV level was established to be $\geq \frac{7}{2}$ from an early study of the $^{13}C(\alpha,n)^{16}O$ reaction.[38] Since this level is excited by an electric quadrupole transition, we may conclude that it has $J^\pi = \frac{7}{2}^+$ or $\frac{9}{2}^+$. Shell-model calculations by Reehal and Wildenthal[31] predict the first two $\frac{7}{2}^+$ levels at 6.77 and 8.40 MeV and the first two $\frac{9}{2}^+$ levels at 8.04 and 10.08 MeV. The state at 8.47 MeV is the most probable candidate for the first $\frac{9}{2}^+$ level, since it has a larger $B(E2\uparrow)$ value than measured for any other state in ^{17}O. We therefore conclude that the most likely J^π assignment for the state at 7.58 MeV is $\frac{7}{2}^+$. Recall also that the weak-coupling-model calculations discussed in the preceding section predict a $\frac{7}{2}^+$ state at 7.56 MeV.

c. The 8.47-MeV level. The level at 8.47 MeV is listed in Ref. 1 as a $\frac{7}{2}^{+}$ state. This assignment is based on the work of Barnes, Belote, and Risser,[39] who investigated the spectroscopy of ^{17}O through studies of the ^{13}C$(\alpha,\alpha)^{13}$C and ^{13}C$(\alpha,n)^{16}$O reactions. Our preferred assignment for this state is $\frac{9}{2}^{+}$. In the following discussion, we review previous works to show that they are consistent with this assignment.

The 8.47-MeV level is excited strongly in the ^{13}C$(\alpha,\alpha)^{13}$C reaction but weakly in the ^{13}C$(\alpha,n)^{16}$O reaction. Thus, $\Gamma_{\alpha} \gg \Gamma_{n}$, where Γ_{α} and Γ_{n} are the alpha-particle and neutron partial widths and $\Gamma \cong \Gamma_{\alpha} + \Gamma_{n}$ is the total width of the level. It was suggested in Ref. 39 that the 8.47-MeV level is excited by $l=3$ alpha particles, which implies that $J^{\pi}=\frac{5}{2}^{+}$ or $\frac{7}{2}^{+}$. The spin assignment of $\frac{7}{2}$ was preferred because of the large magnitudes of both the ^{13}C$(\alpha,\alpha)^{13}$C and ^{13}C$(\alpha,n)^{16}$O cross sections, which are proportional to $(2J+1)(\Gamma_{\alpha}/\Gamma)$ and $(2J+1)(\Gamma_{\alpha}\Gamma_{n})^{1/2}/\Gamma$, respectively. On the other hand, our preferred J^{π} assignment of $\frac{9}{2}^{+}$ implies that this level is excited by $l=5$ alpha particles. It can be inferred from Ref. 39 that all observed states were assumed to be formed with $l \leq 4$. From Fig. 2 of Ref. 40, which was a similar study at higher excitation energies, it can be seen that the angular distribution expected for a $\frac{9}{2}^{+}$ state formed by $l=5$ alpha particles is almost identical to that expected for a $\frac{7}{2}^{+}$ state formed by $l=3$ alpha particles. Thus, we conclude that a $\frac{9}{2}^{+}$ assignment for the 8.47-MeV level is consistent with existing data from the ^{13}C$(\alpha,\alpha)^{13}$C and ^{13}C$(\alpha,n)^{16}$O reactions. A spin assignment of $\frac{7}{2}$ also was proposed for this level from studies of the ^{12}C$(^{7}$Li,d$)^{17}$O and ^{13}C$(^{7}$Li,t$)^{17}$O reactions, based on the assumption that these reactions proceed by the compound-nucleus mechanism.[41]

Our main basis for assigning the 8.47-MeV level to have $J^{\pi}=\frac{9}{2}^{+}$ is its very large $B(E2\uparrow)$ value of 10.1 ± 1.2 e^{2}fm^{4}. This value is more than twice as large as that measured for any other level in ^{17}O. In an oversimplified model that assumes the positive-parity states in ^{17}O arise by "weakly" coupling a $1d_{5/2}$ neutron to the first 2^{+} state of ^{16}O at 6.92 MeV, the $B(E2\uparrow)$ value of a state in ^{17}O with spin J is predicted to be $(2J+1)/30$ times the $B(E2\uparrow)$ value of the 2^{+} state in ^{16}O. For the 6.92-MeV level in ^{16}O, $B(E2\uparrow)=38.9\pm0.2$ e^{2}fm^{4} (Ref. 10). Thus, this model predicts $B(E2\uparrow)=13.0$ e^{2}fm^{4} for the $\frac{9}{2}^{+}$ level in ^{17}O, which agrees reasonably well with our measured value for the 8.47-MeV level. Shell-model calculations by Reehal and Wildenthal[31] also predict the first $\frac{9}{2}^{+}$ level to have a much larger $B(E2\uparrow)$ value than any other level in ^{17}O. Their predicted value of $B(E2\uparrow)=8.2$ e^{2}fm^{4} is also in reasonable agreement with our measured value.

The present assignments for the levels at 5.87, 6.86, 7.58, and 8.47 MeV agree nicely with the predominantly 5p-4h rotational band predicted by the weak-coupling model. Our conclusions regarding these states are supported also by the fact that these states are strongly populated in the ^{12}C$(^{6}$Li,p$)^{17}$O reaction,[42] which should preferentially excite states that contain a large 5p-4h component.
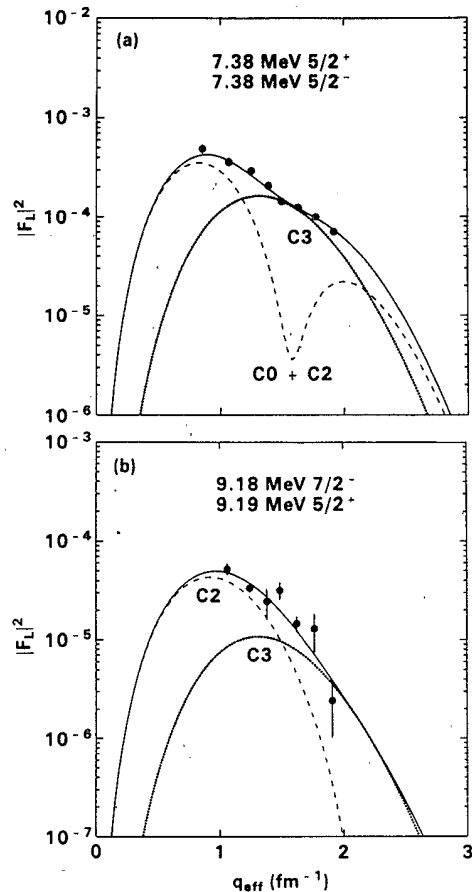

FIG. 7. Longitudinal form factors for (a) the $\frac{5}{2}^{+}$ state in ^{17}O at 7.379 MeV and the $\frac{5}{2}^{-}$ state at 7.382 MeV, and (b) the $\frac{5}{2}^{+}$ state at 9.19 MeV and the $\frac{7}{2}^{-}$ state at 9.18 MeV. See the caption to Fig. 4 for a description of the data points.

2. The levels at 7.38 and 9.19 MeV

The $\frac{5}{2}^{+}$ state at 7.379 MeV was not resolved in our spectra from a narrow $\frac{5}{2}^{-}$ state at 7.382 MeV and the $\frac{5}{2}^{+}$ state at 9.19 MeV was not resolved from a narrow $\frac{7}{2}^{-}$ state at 9.18 MeV. Shown in Figs. 7(a) and 7(b), respectively, are the longitudinal form factors for the doublets at 7.38 and 9.19 MeV. Curves indicate the total contributions from both levels of each doublet. The $\frac{5}{2}^{+}$ level at 7.38 MeV is excited primarily by a monopole transition, whereas the $\frac{5}{2}^{+}$ level at 9.19 MeV is excited primarily by an electric quadrupole transition. The procedure that was used to fit the negative-parity members of both doublets is discussed in Sec. V C.

3. The levels at 6.36, 7.20, 7.96, 8.07, 8.34, and 8.90 MeV

Figures 8(a)–8(d) show the extracted longitudinal form factors for the relatively broad levels at 6.36, 7.20, 7.96, and 8.34 MeV, respectively. Results for these levels should be interpreted with some caution since these states are not easily visible in our measured spectra. Furthermore, the measured form factors for these levels are subject to rather large errors. Reliable form-factor
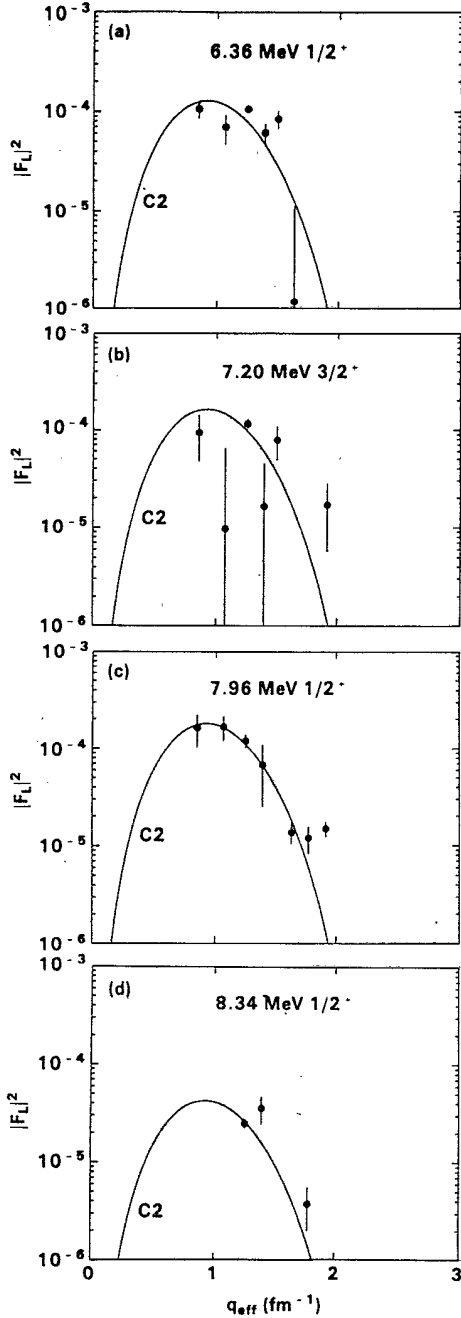
FIG. 8. Longitudinal form factors for weakly excited states in ^{17}O at (a) 6.36 MeV, (b) 7.20 MeV, (c) 7.96 MeV, and (d) 8.34 MeV. The levels at 6.36, 7.96, and 8.34 MeV have $J^{\pi}=\frac{1}{2}^{+}$, whereas the level at 7.20 MeV has $J^{\pi}=\frac{3}{2}^{+}$. See the caption to Fig. 4 for a description of the data points.

measurements could not be obtained for the weakly excited broad levels at 8.07 and 8.90 MeV.

4. Discussion

Only two $\frac{5}{2}^{+}$ states, those at 6.86 and 7.38 MeV, were found to be excited significantly by monopole transitions. The monopole matrix elements $(\mathcal{M})$ for the levels at 6.86 and 7.38 MeV were determined to have values of

TABLE V. $B(E2\uparrow)$ values (in e^{2}fm^{4}) for positive-parity levels in ^{17}O. The present experimental results are compared with the previous low-q electron-scattering measurements of Kim *et al.* (Ref. 5) and with theoretical calculations using the Reehal-Wildenthal (RW) interaction (Ref. 31). Predictions for theoretical levels with an uncertain match with experiment are enclosed in parentheses.

E_x (MeV)	J^{π}	Experiment Present work	Kim *et al.*	Theory RW
0.87	$\frac{1}{2}^{+}$	2.18±0.16	2.10±0.01[a]	2.72
5.09	$\frac{3}{2}^{+}$	2.05±0.20	2.5 ±0.7	
5.87	$\frac{3}{2}^{+}$	2.13±0.22		3.40
6.36	$\frac{1}{2}^{+}$	1.43±0.21	2.1 ±1.3	(0.16)
6.86	$\frac{5}{2}^{+}$	0.83±0.25	1.9 ±1.0	0.01
7.20	$\frac{3}{2}^{+}$	1.79±0.25		(0.79)
7.38	$\frac{5}{2}^{+}$	<0.8		(0.45)
7.58	$\frac{7}{2}^{+}$	4.20±0.51		2.85
7.96	$\frac{1}{2}^{+}$	2.00±0.38		(0.31)
8.34	$\frac{1}{2}^{+}$	0.48±0.07		(0.13)
8.40	$\frac{5}{2}^{+}$	2.10±0.34	8.3 ±2.6	(1.76)
8.47	$\frac{9}{2}^{+}$	10.05±1.19		8.21
9.19	$\frac{5}{2}^{+}$	0.48±0.16		(0.08)

[a]Average of lifetime measurements (Ref. 1).

1.45 ± 0.35 and 3.30 ± 0.31 e fm^2, respectively, where[43]

$$|\mathcal{M}|^{2}=\lim_{q\to\infty}36Z^{2}(F_{C0}/q^{2})^{2} . \tag{14}$$

These values can be compared with $\mathcal{M}=3.46\pm0.18$ e fm^2 for the 0^{+} level in ^{16}O at 6.05 MeV (Ref. 10). Thus, the low-lying monopole strength for ^{17}O is similar to that for ^{16}O. The level at 7.38 MeV contains about 84% of the observed monopole strength for ^{17}O, whereas the level at 6.86 MeV contains about 16% of the total strength.

Extracted $B(E2\uparrow)$ values for the collective and single-particle positive-parity levels in ^{17}O below 9.5 MeV are summarized in Table V. The total $E2$ strength in a given nucleus can be estimated from the sum of $B(E2\uparrow)$ values. For ^{17}O, we obtain $\Sigma B(E2\uparrow)=29.7$ ±1.5 e^{2}fm^{4}, where the sum extends over all states up to 9.5 MeV. This is slightly less than the value of $\Sigma B(E2\uparrow)=38.9\pm0.2$ e^{2}fm^{4} measured for ^{16}O (Ref. 10). Note that only the first 2^{+} state at 6.92 MeV contributes to the sum for ^{16}O in this energy range.

Table V also includes the $B(E2\uparrow)$ values determined from the low-q electron-scattering experiment of Kim *et al.*[5] Uncertainties in the values from the present work are typically much smaller than those from Ref. 5. Theoretical $B(E2\uparrow)$ values calculated with the shell-model code OXBASH,[44] using the interaction of Reehal and Wildenthal,[31] also are included in the table. It was necessary to assume some correspondence between the experimental and calculated energy levels in order to compare the experimental and theoretical $B(E2\uparrow)$

TABLE VI. The positive-parity spectrum of ^{17}O. Experimental excitation energies are compared with theoretical predictions by Reehal and Wildenthal (RW) (Ref. 31) and by Brown and Green (BG) (Ref. 28). Experimental values are from Ref. 1. J^π assignments for levels marked with an asterisk are from the present work. The RW wave functions are given also. Theoretical levels with an uncertain match with experiment are enclosed in parentheses.

$J^\pi)_n$	Excitation energy (MeV)			Wave function (%)		
	Expt.	RW	BG	5p-4h	3p-2h	1p-0h
$\frac{1}{2}^+)_1$	0.87	0.85	0.50	5	34	61
$\frac{1}{2}^+)_2$	6.36	(6.75)	(5.70)	30	62	8
$\frac{1}{2}^+)_3$	7.96	(9.13)	(6.53)	8	90	2
$\frac{1}{2}^+)_4$	8.34	(9.56)	(10.75)	22	78	0
$\frac{3}{2}^+)_1$	5.09		5.10			
$\frac{3}{2}^+)_2$	5.87	4.88	5.71	73	27	0
$\frac{3}{2}^+)_3$	7.20	(7.17)	(6.48)	26	74	0
$\frac{3}{2}^+)_4$	8.07	(7.86)	(7.42)	10	90	0
$\frac{5}{2}^+)_1$	0.00	0.00	0.00	4	28	68
$\frac{5}{2}^+)_2$	6.86*	5.91	7.16	85	12	3
$\frac{5}{2}^+)_3$	7.38	(7.64)	(7.55)	36	59	5
$\frac{5}{2}^+)_4$	8.40	(9.72)	(8.70)	14	86	0
$\frac{7}{2}^+)_1$	7.58*	6.77		76	24	
$\frac{9}{2}^+)_1$	8.47*	8.04		57	43	

values. Such a correspondence is presented in Table VI, which compares the experimental positive-parity levels in ^{17}O with theoretical predictions by Reehal and Wildenthal[31] (RW) and by Brown and Green[28] (BG). The first $\frac{1}{2}^+$, $\frac{3}{2}^+$, and $\frac{5}{2}^+$ states are mainly 1p-0h configurations; the second $\frac{3}{2}^+$ and $\frac{5}{2}^+$ states and first $\frac{7}{2}^+$ and $\frac{9}{2}^+$ states are mainly 5p-4h configurations; the second $\frac{1}{2}^+$ state is mainly a mixture of 3p-2h and 5p-4h configurations.

Calculations similar to those of RW were performed by Zuker, Buck, and McGrory (ZBM).[29] In both calculations, ^{17}O is described in terms of five nucleons moving outside a ^{12}C core. The model space includes all possible configurations of five particles moving in the $1p_{1/2}$, $1d_{5/2}$, and $2s_{1/2}$ orbitals; the $1p_{3/2}$ and $1d_{3/2}$ orbitals are ignored. Consequently, there is no theoretical level that corresponds to the first $\frac{3}{2}^+$ single-particle level. Both calculations treat the single-particle level spacings and two-body matrix elements as free parameters that are determined by fitting shell-model eigenvalues to a selection of experimental energy levels. The wave functions for the theoretical levels at 4.88 MeV ($\frac{3}{2}^+$), 5.91 MeV ($\frac{5}{2}^+$), 6.77 MeV ($\frac{7}{2}^+$), and 8.04 MeV ($\frac{9}{2}^+$) are strongly dominated by the predominantly 5p-4h weak-coupling configurations ^{21}Ne(J^π)$\otimes$ ^{12}C(0^+), where ^{21}Ne(J^π) refers to a state in the ground-state rotational band of ^{21}Ne. Thus, these shell-model calculations support the existence of a $K^\pi = \frac{3}{2}^+$ rotational band in ^{17}O as described in Sec. IV.

The early work of Brown and Green[28] describes positive-parity levels in ^{17}O in terms of a "coexistence model." Physical states are formed by mixing the usual single-particle shell-model states with 3p-2h and 5p-4h deformed states. Thus, unlike the calculations of ZBM and RW, this model includes approximate contributions from the full p and s-d shells.

C. Negative-parity levels

The known negative-parity levels in ^{17}O below 9.50 MeV are listed in Table VII. Peaks were clearly observed in the spectra for the levels at 3.06, 3.84, 4.55, 5.22, 5.38, 5.94, 6.97, 7.17, 7.69, 7.76, 8.90, and 8.97 MeV. Peaks for the strongly excited levels at 5.70 and 5.73 MeV were incompletely resolved and the negative-parity levels at 7.38 and 9.18 MeV were not resolved from the $\frac{5}{2}^+$ levels at 7.38 and 9.19 MeV, respectively.

Form-factor measurements for the negative-parity levels in ^{17}O below 9.50 MeV were fitted with $C1$ and $C3$ components for the longitudinal form factors and with $E1$, $M2$, $E3$, and $M4$ components for the transverse form factors. The shapes of these components were constrained, in part, by fitting form-factor measurements[10,11] for the first 1^- level in ^{16}O at 7.12 MeV, the first 2^- level at 8.87 MeV, the first 3^- level at 6.13 MeV, and the isovector 4^- level at 18.98 MeV. To obtain a good fit for the 1^- level, which has a significant transverse form factor, it is necessary to vary more expansion coefficients for the longitudinal component than are allowed if single-nucleon transitions are confined to the p and s-d shells. Thus, this level probably involves significant transitions to orbitals in the p-f shell. In the momentum-transfer range of this experiment, the $E1$ form factor for the 7.12-MeV level in ^{16}O is larger than the $M2$ form factor for the 8.87-MeV level. Measurements for the first 3^- level in ^{16}O were used only to con-

strain the magnitude of the E3 form factor, which is small, and were not used to constrain the shape of the C3 form factor in ^{17}O.

Values of the oscillator parameter for describing transitions in ^{17}O were not assumed *a priori* to be the same as for describing similar transitions in ^{16}O, except for M4 transitions. The value of the oscillator parameter for describing M2, C3, and E3 form factors in ^{17}O was determined to be 1.818±0.002 fm by simultaneously fitting the levels at 3.06, 5.22, 5.94, 7.76, and 9.15 MeV. These levels cannot be excited by E1 transitions since they have J^π assignments of $\frac{1}{2}^-$, $\frac{9}{2}^-$, or $\frac{11}{2}^-$. Next, the value of the oscillator parameter for describing C1 and E1 form factors was determined to be 1.759±0.018 fm by simultaneously fitting the levels at 3.84, 4.55, 5.38, and 5.70 MeV, which have J^π assignments of $\frac{3}{2}^-$, $\frac{5}{2}^-$, or

TABLE VII. Negative-parity states in ^{17}O below 9.50 MeV. All spins, parities, excitation energies, and widths ($\Gamma > 10$ keV) are from Ref. 1, except where otherwise noted. An asterisk marks levels for which peaks were observed clearly in the measured spectra.

E_x (MeV)	J^π	Γ (keV)	Comments
3.06*	$\frac{1}{2}^-$	<10	
3.84*	$\frac{5}{2}^-$	<10	
4.55*	$\frac{3}{2}^-$	40±5	
5.22*	$\frac{9}{2}^-$	<10	Listed as $(\frac{9}{2}^-)$ in Ref. 1
5.38*	$\frac{3}{2}^-$	28±7	
5.70*	$\frac{7}{2}^-$	<10	
5.73*	$(\frac{5}{2}^-)$	<10	
5.94*	$\frac{1}{2}^-$	32±3	
6.97*	$(\frac{7}{2}^-)$	<10	Listed as $(\frac{5}{2}^+)$ in Ref. 1
7.17*	$\frac{5}{2}^-$	<10	
7.38*	$\frac{5}{2}^-$	<10	Member of unresolved doublet
7.56	$\frac{3}{2}^-$	500±50	
7.69*	$\frac{7}{2}^-$	14.4±0.3	
7.76*	$\frac{11}{2}^-$	<10	
7.99	$\frac{1}{2}^-$	270±30	Not observed in spectra
8.20	$\frac{3}{2}^-$	60	
8.50	$\frac{5}{2}^-$	<10	
8.69	$\frac{3}{2}^-$	55.3±0.6	
8.90^{a}*	$(\frac{9}{2}^-)$	<20	Not listed in Ref. 1
8.97*	$\frac{7}{2}^-$	26±2	
9.15	$\frac{1}{2}^-$	<10	Member of unresolved doublet
9.15	$\frac{9}{2}^-$	<10	Member of unresolved doublet
9.18	$\frac{7}{2}^-$	<10	Member of unresolved doublet
9.42	$\frac{3}{2}^-$	120	
9.49	$\frac{5}{2}^-$	15±1	

^{a}The level we observe at 8.90±0.02 MeV with $\Gamma \leq 20$ keV is probably the level reported in Ref. 39 at 8.884 MeV with $\Gamma = 8$ keV (see text).
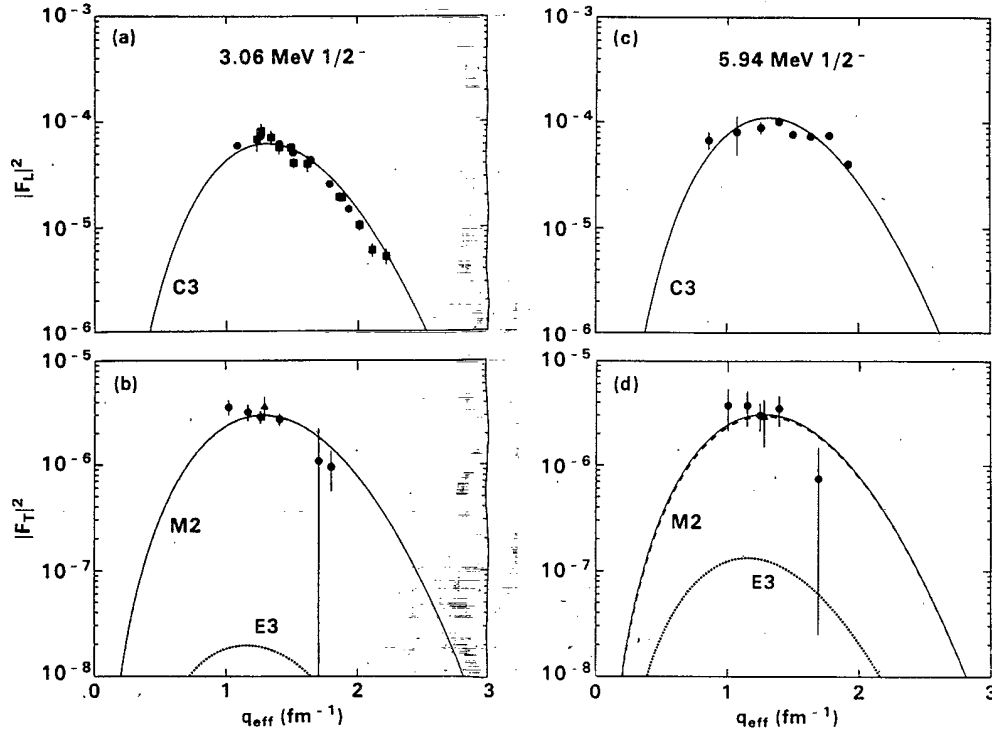
$\frac{7}{2}^-$. The value of the oscillator parameter for M4 form factors in ^{17}O was assumed to be the same (1.58 fm) as for the 18.98-MeV 4$^-$ level in ^{16}O (Ref. 11). We ignored possible M4 transitions in all low-lying levels except those with $J^\pi = \frac{9}{2}^-$ or $\frac{11}{2}^-$. They were considered for these levels because a significant transverse form factor was measured for the $\frac{11}{2}^-$ level at 7.76 MeV that cannot be attributed to E1 or M2 transitions. Further discussion of M4 transitions in ^{17}O can be found in Refs. 8 and 45.

1. The levels with $J^\pi = \frac{1}{2}^-$, $\frac{9}{2}^-$, and $\frac{11}{2}^-$

We consider here the levels at 3.06, 5.22, 5.94, 7.76, 8.90, and 9.15 MeV. The levels in ^{17}O with $J^\pi = \frac{1}{2}^-$, $\frac{9}{2}^-$, and $\frac{11}{2}^-$ are of special interest because their form factors can easily be described empirically: only a C3 component should contribute appreciably to their longitudinal form factors. In contrast, levels with $J^\pi = \frac{3}{2}^-$, $\frac{5}{2}^-$, and $\frac{7}{2}^-$ can be excited by electric dipole transitions and should have longitudinal form factors dominated by C3 and C1 components.

The levels at 3.06 and 5.94 MeV are known[1] to have $J^\pi = \frac{1}{2}^-$. Form factors for these levels are shown in Fig. 9. Both states have significant transverse form factors that are ascribed mainly to M2 transitions. The ZBM wave function[29] for the first $\frac{1}{2}^-$ level is dominated by the ^{20}Ne(0$^+$)⊗^{13}C($\frac{1}{2}^-$) and ^{18}O(0$^+$)⊗^{15}O($\frac{1}{2}^-$) weak-coupling configurations, whereas the ZBM wave function for the second $\frac{1}{2}^-$ level is dominated by the $[^{18}$F(1$^+$)⊗^{15}N($\frac{1}{2}^-$)]$_{1/2^-}$ configuration. Thus, the first $\frac{1}{2}^-$ level in ^{17}O can be described approximately by the wave function $1p_{1/2}$⊗^{16}O(0$_2^+$), where ^{16}O(0$_2^+$) denotes the predominantly 4p-4h state in ^{16}O at 6.05 MeV.

The narrow levels at 7.76 and 9.15 MeV were first observed as selectively excited states in the ^{15}N(α,d)^{17}O reaction.[46] Both levels also are populated strongly in the ^{15}N(^{3}He,p)^{17}O reaction.[34] Wave functions for these levels are probably dominated by the predominantly 2p-1h configurations $[^{18}$F(5$^+$)⊗^{15}N($\frac{1}{2}^-$)]$_{J^\pi}$, where $J^\pi = \frac{9}{2}^-$ or $\frac{11}{2}^-$. The authors of Ref. 46 assumed that the level at 7.76 MeV had $J^\pi = \frac{11}{2}^-$ because of its larger cross section in the ^{15}N(α,d)^{17}O reaction and because shell-model calculations predict the $\frac{11}{2}^-$ state to lie lower in energy than the $\frac{9}{2}^-$ state. Neither level is observed in ^{13}C+α or ^{16}O + n reactions. In the present work, the level at 9.15 MeV was not resolved from a narrow $\frac{1}{2}^-$ level at 9.15 MeV, which has been seen in the ^{13}C(α,α)^{13}C and ^{13}C(α,n)^{16}O reactions.[40]

The narrow level at 5.22 MeV is a strong resonance in the ^{14}N(α,p)^{17}O reaction[47] and was suggested to have $J^\pi = \frac{7}{2}$, $\frac{9}{2}$, or $\frac{11}{2}$ based on the assumption that the reaction proceeds by the compound-nucleus mechanism. This state often is regarded as a strong candidate for the first $\frac{9}{2}^-$ level, which several shell-model calculations predict to lie near 5 MeV. It has not been observed in the ^{13}C+α or ^{16}O + n reactions.

The level at 8.90 MeV is not included in the compila-

FIG. 9. The (a) longitudinal and (b) transverse form factors for the $\frac{1}{2}^-$ state in ^{17}O at 3.06 MeV, and the (c) longitudinal and (d) transverse form factors for the $\frac{1}{2}^-$ state at 5.94 MeV. See the caption to Fig. 4 for a description of the data points.

tion of Ref. 1, although it is listed in an earlier (1971) version[48] as a $\frac{7}{2}^-$ state at 8.87 MeV. Our electron-scattering measurements for this state determine $E_x = 8.90 \pm 0.02$ and $\Gamma \leq 20$ keV. This state is probably the narrow level ($\Gamma_{\text{lab}} = 8$ keV) observed by Barnes, Belote, and Risser[39] at 8.884 MeV in the ^{13}C$(\alpha,\alpha)^{13}$C reaction. Since the level is not seen in the ^{13}C$(\alpha,\text{n})^{16}$O or ^{16}O$(\text{n},\text{n})^{16}$O reactions, it must have $\Gamma \cong \Gamma_\alpha$. Furthermore, since the state is excited by $l = 4$ alpha particles, it must have $J^\pi = \frac{7}{2}^-$ or $\frac{9}{2}^-$. The authors of Ref. 39 assigned the level, rather arbitrarily, to have $J^\pi = \frac{7}{2}^-$. Although the present measurements do not exclude this assignment, we prefer a $\frac{9}{2}^-$ assignment for the level based, in part, upon shell-model arguments. We will return to this point in Sec. V C 2 c.

The present experiment confirms the low-q work of Kim et al.[5] in determining the levels at 5.22 and 7.76 MeV to be excited more strongly by electric octupole transitions than any other levels in ^{17}O. Therefore, these levels must have negative parity and spins between $\frac{1}{2}$ and $\frac{11}{2}$. Shell-model calculations predict only two levels in ^{17}O to have $E3$ strengths comparable to those measured for the levels at 5.22 and 7.76 MeV. One of the levels should be an $\frac{11}{2}^-$ state with a large $[^{18}\text{F}(5^+) \otimes {}^{15}\text{N}(\frac{1}{2}^-)]_{11/2^-}$ component in its wave function; the other level should be a $\frac{9}{2}^-$ state with a large $[^{18}\text{O}(4^+) \otimes {}^{15}\text{O}(\frac{1}{2}^-)]_{9/2^-}$ component. Hence, we confirm that the levels at 7.76 and 9.15 MeV have $J^\pi = \frac{11}{2}^-$ and $\frac{9}{2}^-$, respectively. This follows since the same $\frac{11}{2}^-$ level

that is excited strongly by an octupole transition in electron scattering must be one of the two levels selectively excited in the ^{15}N$(\alpha,\text{d})^{17}$O reaction. Furthermore, we conclude that the level at 5.22 MeV must be the first $\frac{9}{2}^-$ state, which has a large $[^{18}\text{O}(4^+) \otimes {}^{15}\text{O}(\frac{1}{2}^-)]_{9/2^-}$ component in its wave function.

The longitudinal form factor for the $\frac{9}{2}^-$ level at 5.22 MeV is shown in Fig. 10(a). Our $B(E3\uparrow)$ value for this level is larger than that measured for any other level in ^{17}O. Figure 10(b) shows the extracted transverse form factor for the unresolved, weakly excited $\frac{9}{2}^-, \frac{1}{2}^-$ doublet at 9.15 MeV. Contributions from the $M2$, $M4$, and $E3$ components are not well determined; however, any $M4$ component must be associated strictly with the $\frac{9}{2}^-$ level. The longitudinal form factor must be small, since a peak for the doublet was observed more clearly in spectra measured at 160° than at 90°. Figure 10(c) shows the extracted longitudinal form factor for the ($\frac{9}{2}^-$) level at 8.90 MeV. Uncertainties in the form factor are fairly large because this level is excited weakly. The longitudinal form factor for the $\frac{11}{2}^-$ level at 7.76 MeV is shown in Fig. 10(d). The fact that the large well-measured longitudinal form factors for the levels at 5.22 and 7.76 MeV are described very well by a single shape for the $C3$ component provides partial justification of our fitting procedure. Figure 10(e) shows the transverse form factor for the 7.76-MeV level. Its magnitude and shape are consistent with a significant $M4$ component; however, a significant $E3$ component is possible also.
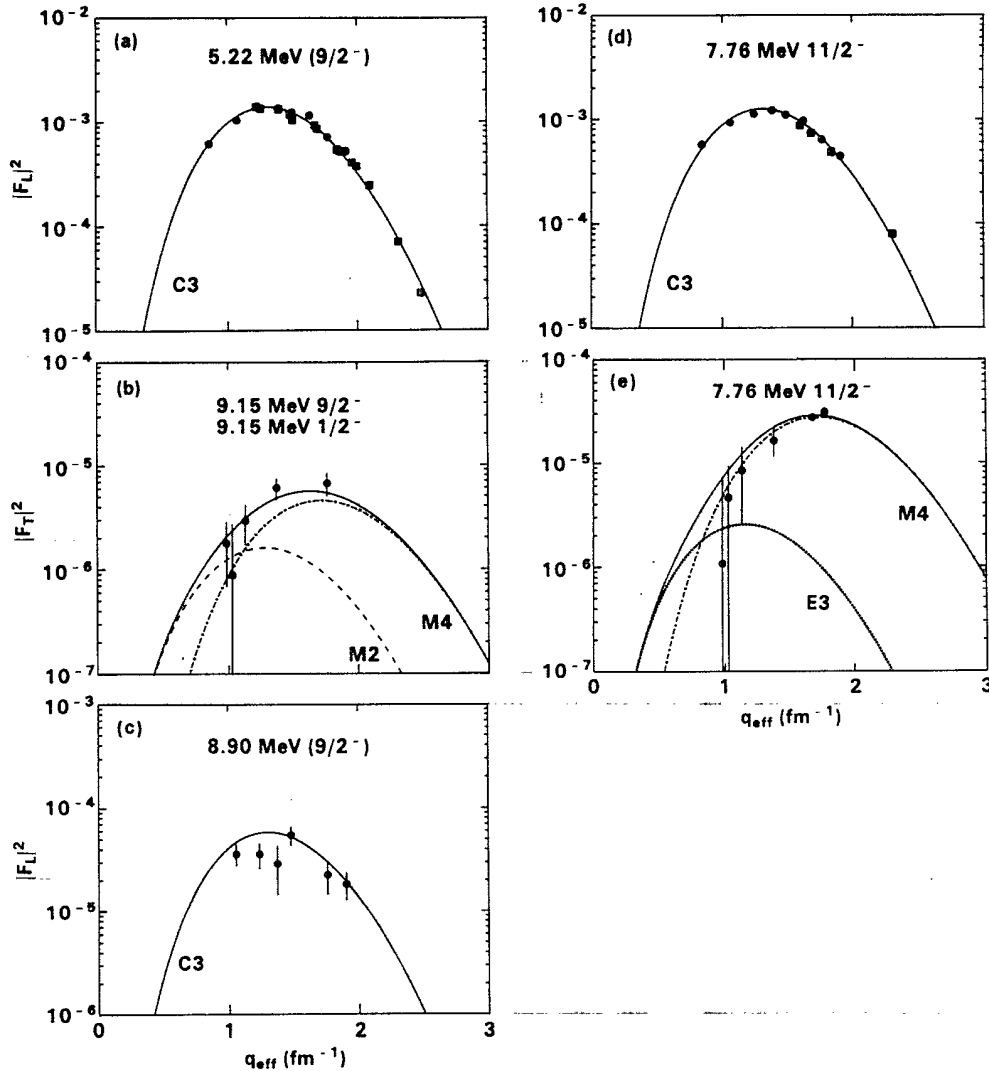
FIG. 10. (a) The longitudinal form factor for the $\frac{9}{2}^-$ state in ^{17}O at 5.22 MeV, (b) the transverse form factor for the unresolved $\frac{1}{2}^-, \frac{9}{2}^-$ doublet at 9.15 MeV, (c) the longitudinal form factor for the $(\frac{9}{2}^-)$ state at 8.90 MeV, and (d) the longitudinal and (e) transverse form factors for the $\frac{11}{2}^-$ state at 7.76 MeV. See the caption to Fig. 4 for a description of the data points.

2. The levels with $J^\pi = \frac{3}{2}^-$, $\frac{5}{2}^-$, and $\frac{7}{2}^-$

The levels considered here are the $\frac{3}{2}^-$ states at 4.55, 5.38, 7.56, 8.20, 8.69, and 9.42 MeV, the $\frac{5}{2}^-$ states at 3.84, 5.73, 7.17, 7.38, 8.50, and 9.49 MeV, and the $\frac{7}{2}^-$ states at 5.70, 6.97, 7.69, 8.97, and 9.18 MeV. Levels in ^{17}O with $J^\pi = \frac{3}{2}^-$, $\frac{5}{2}^-$, and $\frac{7}{2}^-$ can be excited by electric dipole as well as by electric octupole transitions. The $C1$ component in the longitudinal form factor, which peaks at a lower momentum transfer than the $C3$ component, was determined by the deviation from the shape expected for a pure $C3$ transition. For most levels, the $C1$ component is fairly small and not well determined.

a. The $\frac{3}{2}^-$ levels. Strong peaks were seen clearly in the measured spectra for the first two $\frac{3}{2}^-$ states at 4.55 and 5.38 MeV. Peaks for the weakly excited $\frac{3}{2}^-$ states

at 7.56, 8.20, 8.69, and 9.42 MeV were not visually obvious, although an effort was made to extract their cross sections by line-shape fitting. The longitudinal form factors extracted for the levels at 4.55, 5.38, 7.56, 8.20, 8.69, and 9.42 MeV are shown in Figs. 11(a)–11(f), respectively. Since form factors for the weakly excited levels at 8.20 and 8.69 MeV were not well measured, they were fitted ignoring possible contributions from electric dipole transitions.

The shape of the longitudinal form factor for the first $\frac{3}{2}^-$ state at 4.55 MeV suggests a strong $C1$ component. In contrast, the shape for the second $\frac{3}{2}^-$ state at 5.38 MeV suggests dominance by the $C3$ component. The $B(E3\uparrow)$ value determined for the 4.55-MeV level in the present work is 20 ± 12 e^2fm^6, which is considerably less than the value of 98 ± 8 e^2fm^6 determined by the low-q electron-scattering measurements of Kim *et al.*[5] The
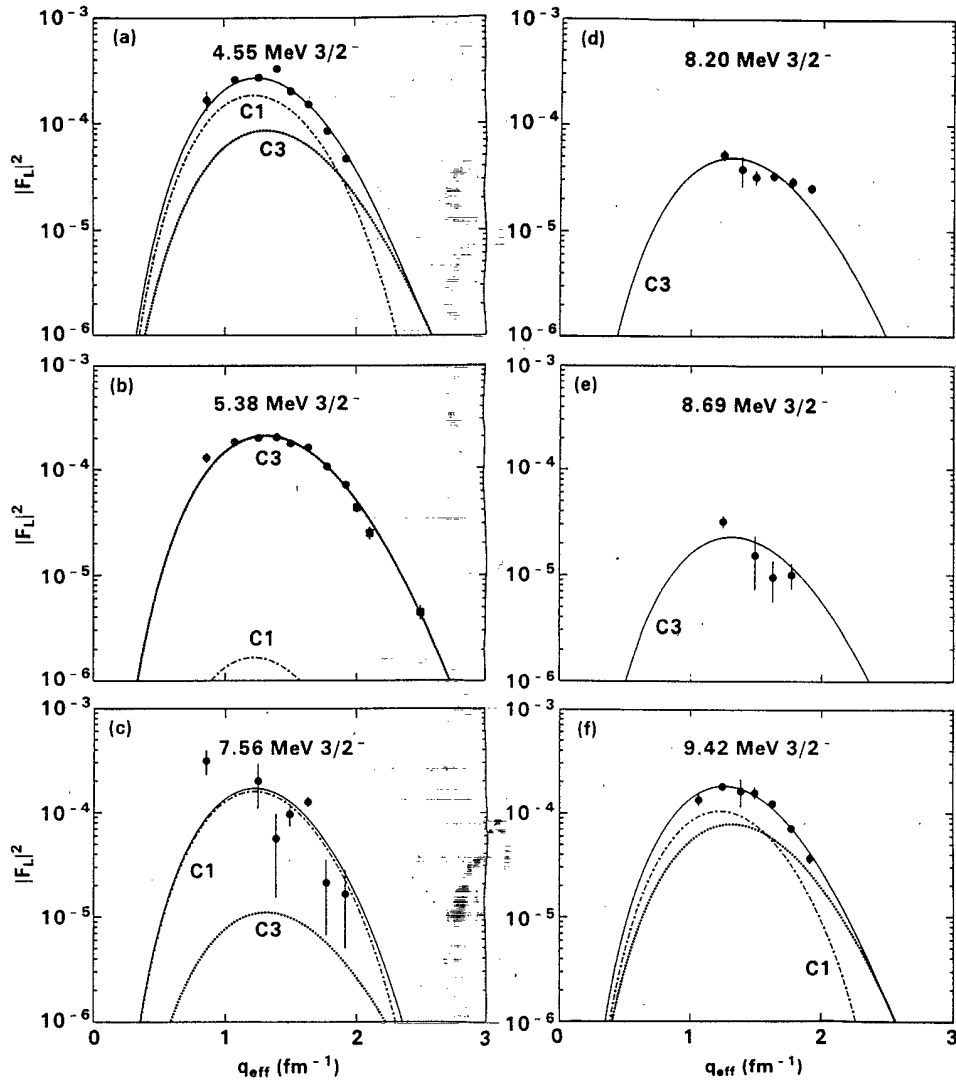
FIG. 11. Longitudinal form factors for the $\frac{3}{2}^-$ states in ^{17}O at (a) 4.55 MeV, (b) 5.38 MeV, (c) 7.56 MeV, (d) 8.20 MeV, (e) 8.69 MeV, and (f) 9.42 MeV. See the caption to Fig. 4 for a description of the data points.

discrepancy stems from the fact that Kim et al. assumed their low-q measurements to be dominated by a $C3$ component, whereas our work suggests that they are probably dominated by a $C1$ component.

The ZBM wave functions[29] for the first two $\frac{3}{2}^-$ levels contain strong admixtures of several predominantly 4p-3h and 2p-1h weak-coupling configurations. Experimentally, a large cross section is observed for the 4.55-MeV level in the ^{13}C(^{6}Li,d)^{17}O reaction,[49] whereas a large cross section is observed for the 5.38-MeV level in the ^{18}O(d,t)^{17}O reaction.[50] Thus, the level at 4.55 MeV is expected to have a predominantly 4p-3h composition, whereas the level at 5.38 MeV is expected to have a predominantly 2p-1h composition. Several shell-model calculations predict a strong $[^{18}$F(1^+)$\otimes^{15}$N($\frac{1}{2}^-$)$]_{3/2^-}$ component for the 5.38-MeV level. The fact that the 5.38-MeV level is excited strongly in the ^{18}O(d,t)^{17}O reaction suggests that the ^{18}O(0^+)$\otimes^{15}$O($\frac{3}{2}^-$) configuration is also a significant component in its wave function.

The extracted longitudinal form factors for the broad $\frac{3}{2}^-$ states at 7.56 MeV ($\Gamma=500$ keV) and 9.42 MeV ($\Gamma=120$ keV) apparently have significant $C1$ components, as does the form factor for the first $\frac{3}{2}^-$ state. Our results for these two broad states should be interpreted with caution, however, since measurements for broad states generally are subject to greater uncertainties than those for narrower states.

b. The $\frac{5}{2}^-$ levels. Longitudinal form factors for the $\frac{5}{2}^-$ levels at 3.84, 5.73, 7.17, 8.50, and 9.49 MeV are shown in Figs. 12(a)–12(e), respectively. The extracted longitudinal form factor for the $\frac{5}{2}^-$ level at 7.38 MeV is shown in Fig. 7(a). This level, as discussed previously, was not resolved from a nearby $\frac{5}{2}^+$ level. The level at 5.73 MeV, which we identify tentatively to have $J^\pi=\frac{5}{2}^-$, was resolved only partially from a $\frac{7}{2}^-$ level at 5.70 MeV. Both levels are excited with about equal strength. Sharp peaks were observed clearly for the isolated $\frac{5}{2}^-$ levels at

3.84 and 7.17 MeV. The level at 8.50 MeV appears in our spectra as a weak shoulder on the strong peak for the positive-parity level at 8.47 MeV. The level at 9.49 MeV is excited weakly and its form factor was not well measured.

The longitudinal form factor for the first $\frac{5}{2}^-$ state at 3.84 MeV was measured particularly well in the present experiment. As shown in Fig. 12(a), it is dominated by a $C3$ component, although a significant $C1$ component is suggested by the enhancement near 1 fm^{-1}. The ZBM wave function[29] for this level is primarily a mixture of the ^{20}Ne(2^+)$\otimes^{13}$C($\frac{1}{2}^-$) and ^{18}O(2^+)$\otimes^{15}$O($\frac{1}{2}^-$) weak-coupling configurations. Thus, the first $\frac{3}{2}^-$ and $\frac{5}{2}^-$ levels in ^{17}O can be described approximately by the wave functions $[1p_{1/2}\otimes^{16}$O(2^+)$]_{J^\pi}$, where $J^\pi=\frac{3}{2}^-$ or $\frac{5}{2}^-$ and ^{16}O(2^+) denotes the predominantly 4p-4h state in ^{16}O at 6.92 MeV.

In the present experiment, the form factor for the level at 5.73 MeV was measured accurately between 0.8 and 1.9 fm^{-1}. This level was not resolved from the $\frac{7}{2}^-$ level at 5.70 MeV in the early electron-scattering experiment of Kim *et al.*[5] Previous spectroscopic studies of ^{17}O have been unable to determine either its spin or parity because of similar problems with low energy resolution. The longitudinal form factor [Fig. 12(b)] for this state is dominated by a $C3$ component; there is no measureable $C1$ component. We conclude that the level has negative parity and a spin between $\frac{1}{2}$ and $\frac{11}{2}$. The large $B(E3\uparrow)$ value of 134 ± 21 e^2fm^6 for this level suggests $J\geq\frac{5}{2}$ and, since shell-model calculations do not predict a low-lying $\frac{9}{2}^-$ or $\frac{11}{2}^-$ state that could correspond to this level, the most likely J^π assignment is $\frac{5}{2}^-$ or $\frac{7}{2}^-$. We prefer a tentative $J^\pi=\frac{5}{2}^-$ assignment for this level, since it is a good candidate for the second $\frac{5}{2}^-$ level that shell-model calculations predict near 6 MeV (see Table VIII).

Measurements for the $\frac{5}{2}^-$ states at 7.17 and 8.50 MeV seem to indicate large $C1$ components in their longitudi-
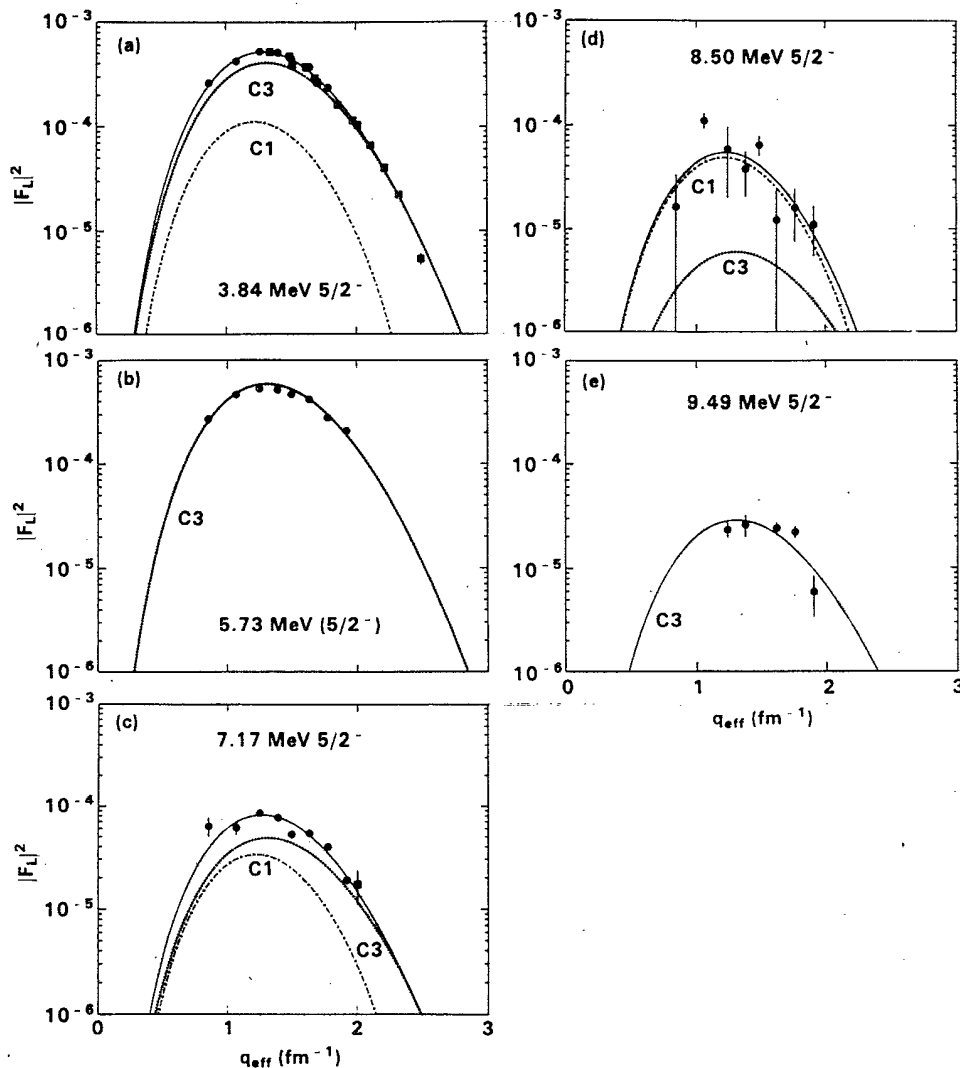

FIG. 12. Longitudinal form factors for the $\frac{5}{2}^-$ states in ^{17}O at (a) 3.84 MeV, (b) 5.73 MeV, (c) 7.17 MeV, (d) 8.50 MeV, and (e) 9.49 MeV. See the caption to Fig. 4 for a description of the data points.

TABLE VIII. The negative-parity spectrum of ^{17}O. Experimental excitation energies are compared with theoretical predictions by Reehal and Wildenthal (RW) (Ref. 31) and by Ellis and Engeland (EE) (Ref. 30). Experimental values are from Ref. 1. J^π assignments for levels marked with an asterisk are from the present work. The RW wave functions are given also. Theoretical levels with an uncertain match with experiment are enclosed in parentheses.

$J^\pi)_n$	Excitation energy (MeV)			Wave function (%)	
	Expt.	RW	EE	4p-3h	2p-1h
$\frac{1}{2}^-)_1$	3.06	3.27	3.1	75	25
$\frac{1}{2}^-)_2$	5.94	6.21	6.3	35	65
$\frac{1}{2}^-)_3$	7.99	(7.53)	(7.4)	29	71
$\frac{1}{2}^-)_4$	9.15	(8.54)	(7.9)	45	55
$\frac{3}{2}^-)_1$	4.55	4.62	(5.0)	59	41
$\frac{3}{2}^-)_2$	5.38	5.80	(6.1)	35	65
$\frac{3}{2}^-)_3$	7.56	(7.74)	(8.3)	38	62
$\frac{3}{2}^-)_4$	8.20	(8.37)	(9.4)	51	49
$\frac{5}{2}^-)_1$	3.84	3.67	5.2	47	53
$\frac{5}{2}^-)_2$	(5.73)*	(6.27)	(7.5)	47	53
$\frac{5}{2}^-)_3$	7.17	(7.85)	(8.1)	49	51
$\frac{5}{2}^-)_4$	7.38	(7.19)	(8.7)	33	67
$\frac{7}{2}^-)_1$	5.70	6.02	6.4	24	76
$\frac{7}{2}^-)_2$	(6.97)*	(8.08)	(8.2)	41	59
$\frac{7}{2}^-)_3$	7.69	(8.45)		43	57
$\frac{7}{2}^-)_4$	8.97	(9.44)	(9.44)	83	17
$\frac{9}{2}^-)_1$	5.22*	5.39	6.7	31	69
$\frac{9}{2}^-)_2$	(8.90)*	(9.34)		95	5
$\frac{9}{2}^-)_3$	9.15	8.08	9.1	23	77
$\frac{11}{2}^-)_1$	7.76	7.23	7.3	23	77

nal form factors. The longitudinal form factor for the 8.50-MeV level, in particular, seems to be dominated by the $C1$ component. These results again must be interpreted with caution, since the measured form factors for these levels have fairly large uncertainties. Form factors for the levels at 7.38 and 9.49 MeV were fitted ignoring possible contributions from dipole transitions. Hence, the $B(E3\uparrow)$ values extracted for these levels should be regarded as upper limits.

c. The $\frac{7}{2}^-$ levels. Longitudinal form factors for the $\frac{7}{2}^-$ levels at 5.70, 6.97, 7.69, and 8.97 MeV are shown in Figs. 13(a)–13(d), respectively. The extracted longitudinal form factor for the $\frac{7}{2}^-$ level at 9.18 MeV is shown in Fig. 7(b). This level was not resolved from the $\frac{5}{2}^+$ state at 9.19 MeV. We tentatively assign $J^\pi = \frac{7}{2}^-$ to the level at 6.97 MeV. The spins and parities of the levels at 5.70, 7.69, and 8.97 MeV were established from early studies of the ^{16}O + n and ^{13}C + α reactions.[36–38,51]

The longitudinal form factors for the $\frac{7}{2}^-$ states at 5.70, 6.97, 7.69, and 8.97 MeV are dominated by $C3$ components, although significant $C1$ components seem to be indicated for the levels at 6.97 and 8.97 MeV. Possible dipole contributions were ignored for the $\frac{7}{2}^-$ level at 9.18 MeV.

The ZBM wave functions[29] for the first $\frac{7}{2}^-$ level (5.70

MeV) and the third $\frac{5}{2}^-$ level (7.17 or 7.38 MeV) are dominated by the predominantly 2p-1h weak-coupling configuration $[^{18}F(3^+)\otimes {}^{15}N(\frac{1}{2}^-)]_{J^\pi}$, where $J^\pi = \frac{5}{2}^-$ or $\frac{7}{2}^-$. Shell-model calculations by Ellis and Engeland[30] and Millener[45] predict a similar structure for the first $\frac{7}{2}^-$ state. The ZBM wave functions[29] for the fourth $\frac{7}{2}^-$ level (8.97 MeV?) and the third $\frac{9}{2}^-$ level (8.90 MeV?) are similarly dominated by the predominantly 4p-3h weak-coupling configuration $[^{20}Ne(4^+)\otimes {}^{13}C(\frac{1}{2}^-)]_{J^\pi}$, where $J^\pi = \frac{7}{2}^-$ or $\frac{9}{2}^-$. Thus, the levels in ^{17}O at 8.97 and 8.90 MeV are candidates for states that can be described approximately by the configurations $[1p_{1/2}\otimes {}^{16}O(4^+)]_{J^\pi}$, where $^{16}O(4^+)$ denotes the predominantly 4p-4h state in ^{16}O at 10.36 MeV and $J^\pi = \frac{7}{2}^-$ or $\frac{9}{2}^-$. If the level at 8.90 MeV has $J^\pi = \frac{7}{2}^-$, as suggested by the authors of Ref. 39, then it is difficult to match it with one of the theoretical levels calculated by ZBM.[29] It should be noted that the ZBM model is quite successful at predicting excitation energies. If, on the other hand, the level at 8.90 MeV has $J^\pi = \frac{9}{2}^-$, which is our preferred assignment, then it probably corresponds to the third ZBM level at 9.03 MeV. The large $^{20}Ne(4^+)\otimes {}^{13}C(\frac{1}{2}^-)$ component in the wave function of that state also offers a possible explanation for the large cross section of the
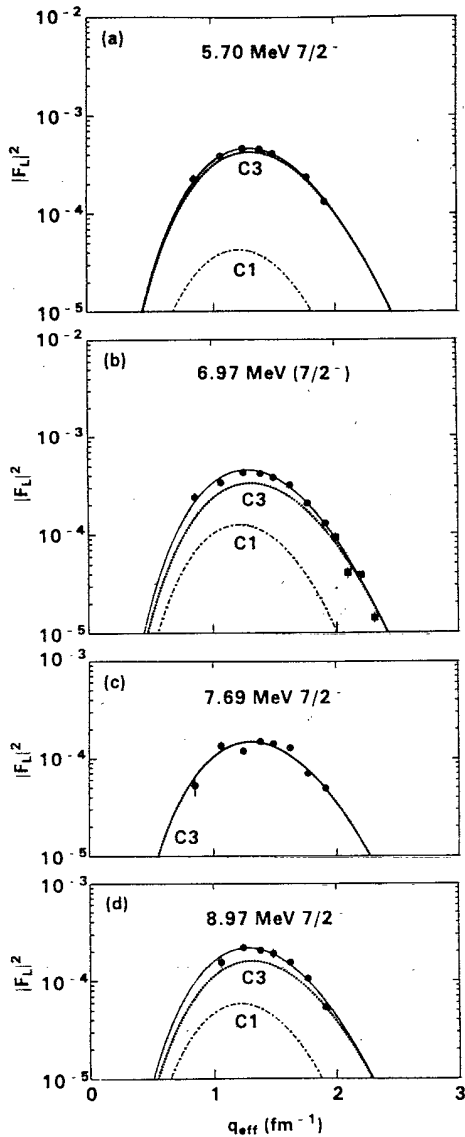
FIG. 13. Longitudinal form factors for the $\frac{7}{2}^-$ states in ^{17}O at (a) 5.70 MeV, (b) 6.97 MeV, (c) 7.69 MeV, and (d) 8.97 MeV. See the caption to Fig. 4 for a description of the data points.

8.90-MeV level in the ^{13}C$(\alpha,\alpha)^{13}$C reaction.[39]

The spin and parity of the level at 6.97 MeV were not established from prior experiments. A tentative J^π assignment of $\frac{5}{2}^+$ was suggested, however, from a study of the ^{15}N$(^3$He,p$)^{17}$O reaction.[34] A spin of $\frac{7}{2}$ also was suggested from studies of the ^{12}C$(^7$Li,d$)^{17}$O and ^{13}C$(^7$Li,t$)^{17}$O reactions, where it was assumed that these reactions proceed by the compound-nucleus mechanism.[41] The present work suggests strongly that the 6.97-MeV level is excited by electric octupole and dipole transitions, which implies that it has $J^\pi = \frac{3}{2}^-$, $\frac{5}{2}^-$, or $\frac{7}{2}^-$. Experimental candidates exist for all of the low-lying $\frac{5}{2}^-$ states predicted by shell-model calculations. However, the 6.97-MeV level is clearly a candidate for the second $\frac{5}{2}^-$ state predicted near 5 MeV, which we have discussed already. Shell-model calculations also predict a second

$\frac{7}{2}^-$ state near 7 or 8 MeV, which may correspond to the 6.97-MeV level or the known $\frac{7}{2}^-$ level at 7.69 MeV. In a study[34] of the ^{15}N$(^3$He,p$)^{17}$O reaction, it was discovered than the measured angular distribution for the 7.69-MeV level could be described by the ZBM wave function[29] for the third, but not the second, theoretical $\frac{7}{2}^-$ level. These results suggest that the 6.97-MeV is a good candidate for the second $\frac{7}{2}^-$ level predicted by the ZBM model. Since the level at 5.73 MeV is our preferred candidate for the second $\frac{5}{2}^-$ level, we *tentatively* assign $J^\pi = \frac{7}{2}^-$ to the level at 6.97 MeV.

3. Discussion

The experimental negative-parity spectrum of ^{17}O below 9.5 MeV is compared in Table VIII with theoretical calculations by Reehal and Wildenthal[31] (RW) and by Ellis and Engeland[30] (EE). The calculations by RW, which have been discussed already, are similar to those of ZBM (Ref. 29) and Bobker.[52] Calculations by EE were performed within the framework of a weak-coupling model restricted to the p and s-d shells. In their model, negative-parity particle-hole configurations lying above 9 MeV were neglected and wave functions were restricted to have a maximum of five components. While still an approximate treatment, the EE model allows for particles and holes in the $1p_{3/2}$ and $1d_{3/2}$ orbitals, which are not active in calculations by Bobker, ZBM, and RW. General agreement with experiment among the various theoretical calculations is quite reasonable. We have not attempted to compare experimental energy levels with the predictions of theoretical calculations[45,53] that are restricted to 2p-1h configurations, since there is ample experimental and theoretical evidence to indicate the importance of 4p-3h configurations in the low-lying negative-parity states.

Knowledge of the theoretical wave functions often is required to match the theoretical and experimental energy levels. In several cases where levels with the same J^π lie near in energy (less than about 2 MeV), the ordering of theoretical levels may be inverted relative to the experimental levels. We have attempted in our discussion to indicate some cases where such level inversions may occur.

In Table IX we compare experimental $B(E3\uparrow)$ values determined by the present experiment with those determined by the low-q electron-scattering experiment of Kim *et al.*[5] The value of the oscillator parameter in Ref. 5, $b = 1.83 \pm 0.10$ fm, is in good agreement with the value $b = 1.818 \pm 0.002$ fm, determined for octupole excitations in the present work. Uncertainties are smaller than in Ref. 5 for several of the levels studied in both experiments. The average agreement between this work and Ref. 5 is only about 40%, however, which is much poorer than would be expected from the quoted experimental uncertainties. An inspection of Table IX reveals that the $B(E3\uparrow)$ values determined in the present work are systematically lower than those in Ref. 5. The disagreement can be attributed, in part, to the absence of $E1$ strength in Ref. 5. The similarity in shapes of the $C1$

TABLE IX. $B(E3\uparrow)$ values (in $e^2\text{fm}^6$) for negative-parity levels in ^{17}O. The present experimental results are compared with the previous low-q electron-scattering measurements of Kim et al. (Ref. 5) and with theoretical predictions calculated with the models of Reehal and Wildenthal (RW) (Ref. 31) and Millener (Ref. 45). Predictions for theoretical levels with an uncertain match with experiment are enclosed in parentheses.

E_x (MeV)	J^π	Experiment Present work	Experiment Kim et al.	Theory RW	Theory Millener
3.06	$\frac{1}{2}^-$	14.1±3.9	31±6	4	31
3.84	$\frac{5}{2}^-$	93.0±8.3	153±6	83	116
4.55	$\frac{3}{2}^-$	20±12	98±8	27	46
5.22	$\frac{9}{2}^-$	319±13	360±11	337	324
5.38	$\frac{3}{2}^-$	47.9±4.3	45±12	49	50
5.70	$\frac{7}{2}^-$	97.0±6.5	270±32	117	131
5.73	$(\frac{5}{2}^-)$	134±21		(97)	(61)
5.94	$\frac{1}{2}^-$	25.3±5.1	17±10	16	
6.97	$(\frac{7}{2}^-)$	75.5±5.6	147±34	(16)	(78)
7.17	$\frac{5}{2}^-$	11.1±2.9	22±25	(<1)	
7.38	$\frac{5}{2}^-$	36.9±2.4	47±38	(10)	
7.56	$\frac{3}{2}^-$	<15		(20)	
7.69	$\frac{7}{2}^-$	33.9±4.9		(1)	(101)
7.76	$\frac{11}{2}^-$	287±14	369±15	314	290
8.20	$\frac{3}{2}^-$	11.0±1.3		(<1)	
8.50	$\frac{5}{2}^-$	<7		(1)	
8.69	$\frac{3}{2}^-$	5.2±1.2		(<1)	
8.90	$(\frac{9}{2}^-)$	13.3±2.3		(8)	
8.97	$\frac{7}{2}^-$	36.3±4.1		(27)	
9.15	$\frac{1}{2}^-$	<2.3		(3)	
9.15	$\frac{9}{2}^-$			<1	
9.18	$\frac{7}{2}^-$	2.4±1.0			
9.42	$\frac{3}{2}^-$	17.6±4.8			
9.49	$\frac{5}{2}^-$	6.5±1.0			

and $C3$ form factors cause difficulty in separating contributions from these multipoles. Reliable extraction of the $C1$ component requires measurements, with high statistics, of the form factor at momentum transfers near the photon point.

The reliability of our $B(E3\uparrow)$ values for ^{17}O can be estimated by using the polynomial-times-Gaussian approximation [Eq. (9)] to fit recent form-factor measurements of Buti et al.[10] for the first 3^- level in ^{16}O at 6.13 MeV. The resulting $B(E3\uparrow)$ value agrees to within 10% with the model-independent value in Ref. 10, which was obtained by including additional low-q measurements in the fit.

The total $E3$ strength for ^{17}O measured in Ref. 5 (see Table IX) is $\Sigma B(E3\uparrow)=1559\pm70$ $e^2\text{fm}^6$, where the sum extends over all states up to 8 MeV. In the same region the present experiment determines $\Sigma B(E3\uparrow)=1400\pm34$ $e^2\text{fm}^6$, whereas if the integration region is extended to 9.5 MeV, we obtain $\Sigma B(E3\uparrow)=1619\pm35$ $e^2\text{fm}^6$. To compare with ^{16}O, we note that $B(E3\uparrow)=1411\pm28$ $e^2\text{fm}^6$ for the first 3^- state in ^{16}O at 6.13 MeV (Ref. 10),

which is the only low-lying 3^- state in ^{16}O. We conclude that, while ^{16}O and ^{17}O have comparable $E3$ strengths, there may be as much as 15% more low-lying $E3$ strength for ^{17}O than for ^{16}O.

Table IX also compares the experimental $B(E3\uparrow)$ values with theoretical predictions calculated with the shell-model code OXBASH,[44] using the Reehal-Wildenthal (RW) interaction as described in Ref. 31, and with Millener's model,[45] which includes all possible 2p-1h configurations within a $1\hbar\omega$ basis. The theoretical $B(E3\uparrow)$ values labeled "Millener" in Table IX were calculated from the isoscalar and isovector matrix elements in Ref. 45. We used an oscillator parameter of $b=1.818$ fm, which was determined from our electron-scattering measurements, and polarization charges of $\delta_p^p=0$ and $\delta_p^n=0.42$, where δ_p^p and δ_p^n describe the polarization of core protons by valence protons and neutrons, respectively.[45] Both sets of theoretical $B(E3\uparrow)$ values generally agree very well with the results of the present experiment. Since the first $\frac{9}{2}^-$ level at 5.22 MeV and the first $\frac{11}{2}^-$ level at 7.76 MeV are believed to be dominated by

TABLE X. States in ^{17}O between 9.5 and 15 MeV. All spins, parities, excitation energies, and widths ($\Gamma > 10$ keV) are from Ref. 1, except where otherwise noted. An asterisk marks levels with $T = \frac{3}{2}$.

E_x (MeV)	J^π	Γ (keV)	Comments
9.71	$\frac{7}{2}^+$	23.1±0.3	
9.86	$(\frac{5}{2}^-)$	<10	Unresolved doublet
9.88	$(\frac{1}{2}^-)$	16.7±1.7	
11.04		31 ±3	Unresolved doublet
11.08*	$\frac{1}{2}^-$	<10	
12.22		<20	Not listed in Ref. 1
12.47*	$\frac{3}{2}^-$	<10	
12.94*	$\frac{1}{2}^+$	<10	Unresolved doublet
13.00*	$\frac{5}{2}^-$	<10	
13.58	$(\frac{11}{2}^-)$	68 ±19	Width from present work
14.23*	$\frac{7}{2}^-$	20.5±1.6	Listed as $(\frac{7}{2}^-)$ in Ref. 1
14.45		40 ±6	
14.72*	$\frac{9}{2}^-$	35 ±11	Not listed in Ref. 1

2p-1h configurations, it is particularly gratifying that our experimental results for these levels are reproduced by Millener's model. It should be noted, however, that $\delta_p^p < \delta_p^n$ is required in order for this model to reproduce the slightly smaller $B(E3\uparrow)$ value of the $\frac{11}{2}^-$ level. The principal cases of strong disagreement between the two

theoretical calculations are for the second and third $\frac{7}{2}^-$ levels. Measured $B(E3\uparrow)$ values of the corresponding experimental levels do not agree better with one calculation than the other.

The measured transverse form factors for the negative-parity states in ^{17}O are generally small and typically have large uncertainties in both this work and in Ref. 5. Transverse form factors of the $\frac{1}{2}^-$ level at 3.06 and 5.94 MeV (see Fig. 9) are expected to be *dominated* by $M2$ components. In addition to these two $\frac{1}{2}^-$ levels, several states with $J^\pi = \frac{3}{2}^-$ and $\frac{5}{2}^-$, and $\frac{7}{2}^-$ appear to have significant $M2$ strength. The levels at 5.70 and 7.38 MeV, in particular, appear to have large $M2$ form factors. Unfortunately, credible $B(M2\uparrow)$ and $B(E1\uparrow)$ values could not be extracted due to lack of high-statistics data at sufficiently low momentum transfers.

D. The levels between 9.5 and 15 MeV

Table X lists the levels in ^{17}O between 9.5 and 15 MeV for which peaks were observed clearly in the measured spectra. Several of these levels are evident in Fig. 14, which show a ^{9}Be^{17}O spectrum measured at 90° for an incident energy of 268.8 MeV. Particularly obvious are the predominantly 2p-1h states with $T = \frac{3}{2}$ at 12.47 MeV ($\frac{3}{2}^-$), 13.00 MeV ($\frac{5}{2}^-$), 14.23 MeV ($\frac{7}{2}^-$), and 14.72 MeV ($\frac{9}{2}^-$), and the narrow state at 12.22 MeV, which has not been reported previously. Shown in Fig. 15 are total form-factor measurements for the levels we observed at (a) 9.71 MeV, (b) 9.86 and 9.88 MeV, (c) 11.04
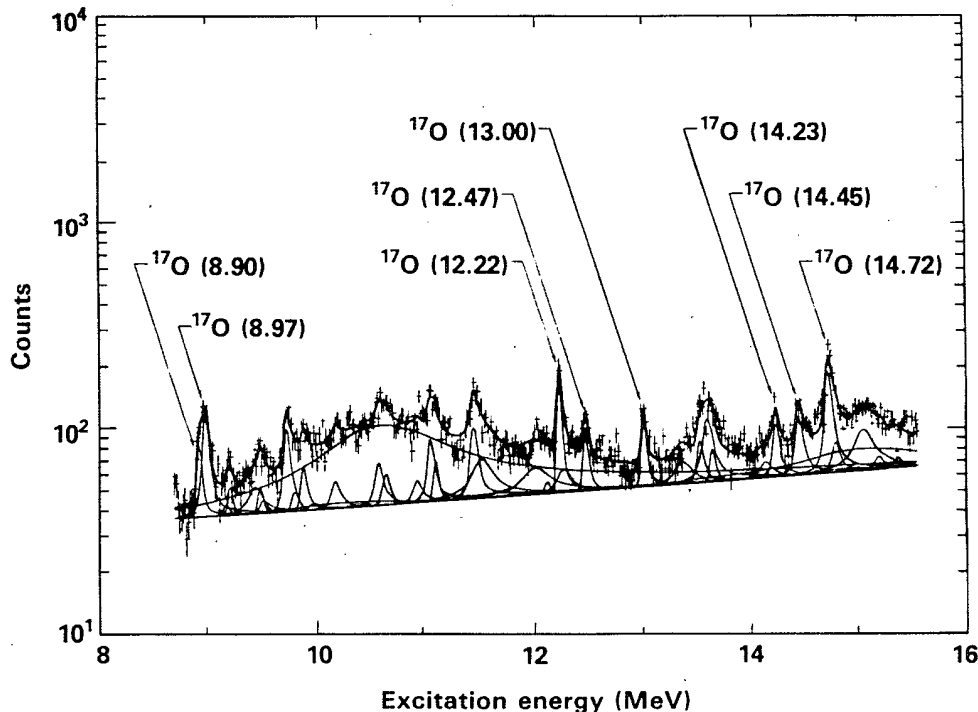

FIG. 14. Part of a fitted electron spectrum for ^{9}Be^{17}O measured at $\theta=90°$ for $E_0=268.8$ MeV. The curves show the results of both the overall fit and contributions from individual peaks. Note, particularly, the new state at 12.22 MeV and the $T = \frac{3}{2}$ states at 12.47, 13.00, 14.23, and 14.72 MeV. The broad peak near 10.5 MeV is a state in ^{9}Be.

and 11.08 MeV, (d) 12.22 MeV, (e) 12.47 MeV, (f) 12.94 and 13.00 MeV, (g) 13.58 MeV, (h) 14.23 MeV, (i) 14.45 MeV, and (j) 14.72 MeV. Total form-factor measurements at 90° and 160° are displayed as solid circles and squares, respectively. Measurements in this excitation region were too sparse to separate longitudinal and transverse components except at a few values of momentum transfer.

The level at 9.71 MeV is listed in Ref. 1 as a $\frac{7}{2}^+$ state. This J^π assignment was determined from a study of the $^{13}C(\alpha,\alpha)^{13}C$ and $^{13}C(\alpha,n)^{16}O$ reactions.[40] Present electron-scattering measurements for this state [Fig.
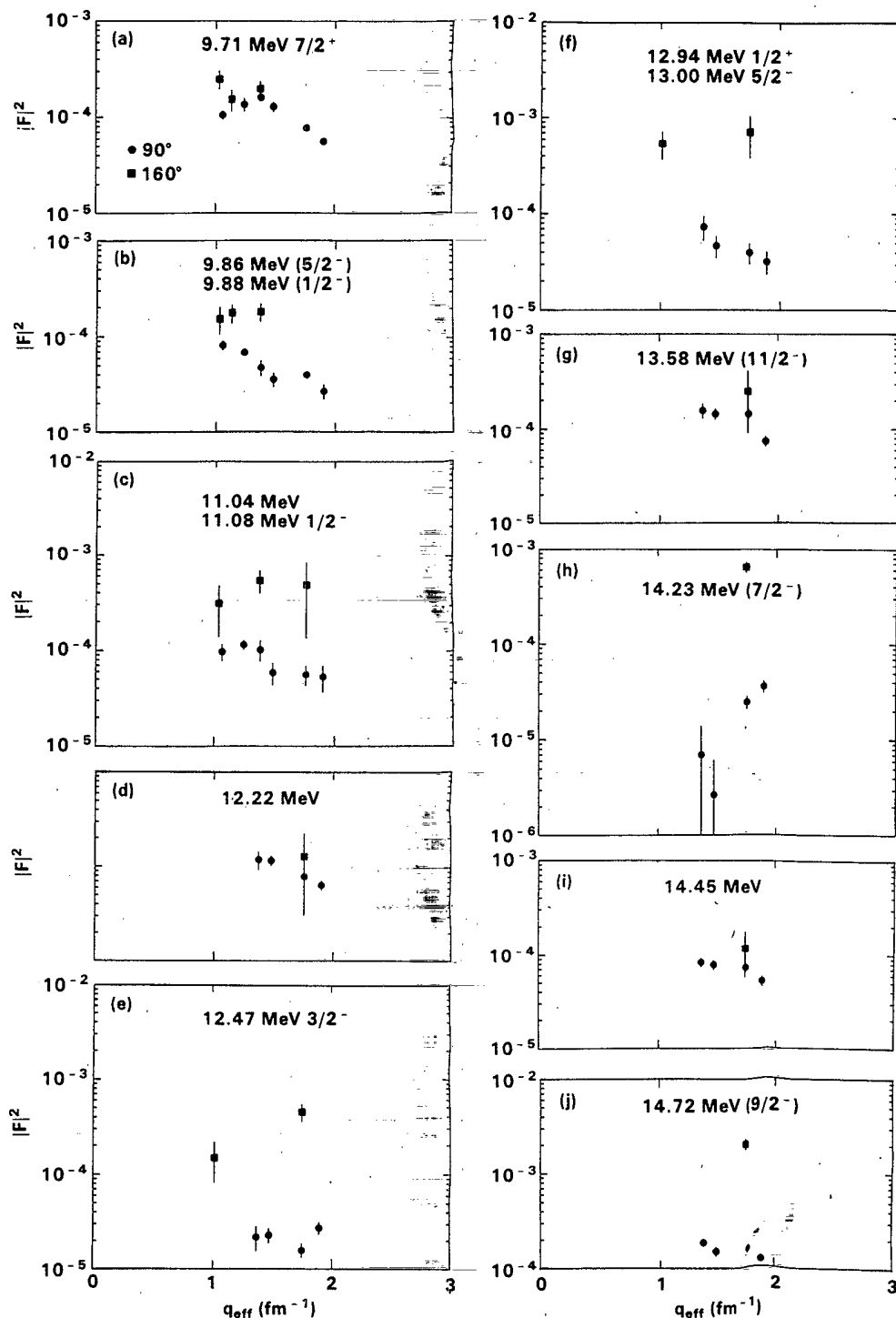

FIG. 15. Total form factors for the states in ^{17}O at (a) 9.71 MeV, (b) 9.86 and 9.88 MeV, (c) 11.04 and 11.08 MeV, (d) 12.22 MeV, (e) 12.47 MeV, (f) 12.94 and 13.00 MeV, (g) 13.58 MeV, (h) 14.23 MeV, (i) 14.45 MeV, and (j) 14.72 MeV. Measurements at 90° and 160° are shown as solid circles and squares, respectively.

15(a)] indicate that its transverse form factor is small. If its positive-parity assignment is correct, then its form factor is probably dominated by a strong $C4$ component. It should be noted that significant $E4$ strength is not expected in ^{17}O at excitation energies below about 9.5 MeV.

The unresolved levels at 9.86 and 9.88 MeV have tentative J^π assignments of $\frac{5}{2}^-$ and $\frac{1}{2}^-$, respectively, which were suggested by a high-resolution study of the $^{16}O(n,n)^{16}O$ reaction.[54] Our electron-scattering measurements for this doublet [Fig. 15(b)] indicate a significant transverse form factor.

The unresolved levels at 11.04 and 11.08 MeV have $T = \frac{1}{2}$ and $\frac{3}{2}$, respectively. The spin and parity of the 11.04-MeV state are unknown. However, J^π for the 11.08-MeV state, which is the first level in ^{17}O to have $T = \frac{3}{2}$, is well established to be $\frac{1}{2}^-$. As indicated in Table III, this level is dominated by the predominantly 2p-1h weak-coupling configuration $^{18}O(0^+) \otimes {}^{15}O(\frac{1}{2}^-)$. Figure 15(c) indicates that, within experimental uncertainties, the form factor for the unresolved doublet is completely transverse.

A new level was observed at $E_x = 12.22 \pm 0.02$ MeV with $\Gamma \leq 20$ keV. This level is very near the energy (12.32 MeV) predicted for the predominantly 4p-3h configuration $[^{20}Ne(4^+) \otimes {}^{13}C(\frac{3}{2}^-)]_{J\pi}$, where $J^\pi = \frac{5}{2}^-$, $\frac{7}{2}^-$, $\frac{9}{2}^-$, or $\frac{11}{2}^-$. Our measurements [Fig. 15(d)] for the 12.22-MeV level suggest that its transverse form factor is probably small.

The levels at 12.47 and 13.00 MeV have $J^\pi = \frac{3}{2}^-$ and $\frac{5}{2}^-$, respectively. Both levels have $T = \frac{3}{2}$ and are dominated (see Table III) by the predominantly 2p-1h weak-coupling configurations, $[^{18}O(2^+) \otimes {}^{15}O(\frac{1}{2}^-)]_{J\pi}$, where $J^\pi = \frac{3}{2}^-$ or $\frac{5}{2}^-$. The level at 13.00 MeV probably corresponds to an isolated narrow peak that we observed at 12.97 ± 0.02 MeV, although this peak may contain contributions from the narrow $\frac{1}{2}^+$ state with $T = \frac{3}{2}$ at 12.94 MeV. We regard this possibility as unlikely, however, since no other established positive-parity states with $T = \frac{3}{2}$ were observed to be excited strongly in our spectra. The form factors for the peaks we observed at 12.47 and 12.97 MeV [Figs. 15(e) and 15(f), respectively] appear to have large transverse components.

The level at 13.58 MeV is selectively excited in the $^{13}C(^6Li,d)^{17}O$ and $^{13}C(^7Li,t)^{17}O$ reactions.[49] This level was suggested to have $J^\pi = \frac{11}{2}^-$ or $\frac{13}{2}^-$, based on the assumption that it is dominated by the predominantly 4p-3h configuration $1p_{1/2} \otimes {}^6O(6^+)$, where $^{16}O(6^+)$ refers to the mainly 4p-4h state in ^{16}O at 16.28 MeV. In the notation of Sec. IV, its wave function should be dominated by $[^{20}Ne(6^+) \otimes {}^{13}C(\frac{1}{2}^-)]_{J\pi}$, where $^{20}Ne(6^+)$ denotes the first 6^+ level in ^{20}Ne at 8.78 MeV. Our calculated excitation energy for this configuration is 13.17 MeV, where we used the parameters $A = 0.23$ MeV and $B = 5.02$ MeV from Sec. IV. The level observed in our spectra has $E_x = 13.58 \pm 0.02$ MeV and $\Gamma = 68 \pm 19$ keV. Our electron-scattering measurements [Fig. 15(g)] suggest that its transverse form factor is small. Therefore, we regard the suggested $\frac{13}{2}^-$ assignment as unlikely and we

tentatively assign this level to have $J^\pi = \frac{11}{2}^-$.

The levels at 14.23 and 14.72 MeV have $J^\pi = \frac{7}{2}^-$ and $\frac{9}{2}^-$, respectively. Both levels have $T = \frac{3}{2}$ and are assumed to be. dominated by the predominantly 2p-1h weak-coupling configurations $[^{18}O(4^+) \otimes {}^{15}O(\frac{1}{2}^-)]_{J\pi}$, where $J^\pi = \frac{7}{2}^-$ or $\frac{9}{2}^-$. The form factors for these levels are dominated by transverse components, as shown in Figs. 15(h) and 15(j). The level that we observe at $E_x = 14.72 \pm 0.02$ MeV was measured to have total width $\Gamma = 35 \pm 11$ keV. This level corresponds to the level recently observed at 14.75 MeV in the low-q electron-scattering measurements of Ref. 7. Thus, our experiment independently confirms its existence. The $\frac{9}{2}^-$ assignment for the 14.72-MeV level is based, in part, on its very large transverse form factor, which probably has a significant $E3$ component. It should be noted that our measured excitation energy for this level agrees perfectly with a calculation of Hinterberger *et al.*,[55] which used the isobaric-mass-multiplet equation.

The final level in this energy range that we discuss is the state at 14.45 MeV. Its spin, parity, and isospin were not established previously, although it was observed in high-resolution measurements of the $^{16}O(n,n)^{16}O$ reaction.[55] Our electron-scattering measurements [Fig. 15(i)] for this level indicate that its transverse form factor is small.

The measured form factors for all ^{17}O states discussed in this paper, including previously unpublished data from Ref. 12, and their fitted expansion coefficients [see Eq. (9)] may be obtained from the Physics Auxiliary Publication Service (PAPS).[56]

VI. SUMMARY AND CONCLUSIONS

We have presented the results of an extensive new study of ^{17}O by inelastic electron scattering. Nine excited states below 9.5 MeV with positive parity and 15 states with negative parity were observed clearly in the measured spectra. Most of these states have relatively narrow widths ($\Gamma \leq 40$ keV).

The present work may be regarded as a spectroscopic study since our approach has been motivated, in large part, by an effort to determine or constrain the spins and parities of several levels whose previous J^π assignments were uncertain or unknown. On the basis of the theoretical and experimental results discussed in this paper, the levels at 5.22, 6.86, 7.58, and 8.47 MeV are assigned J^π values of $\frac{9}{2}^-$, $\frac{5}{2}^+$, $\frac{7}{2}^+$, and $\frac{9}{2}^+$, respectively. We determine the parities of the levels at 5.73 and 6.97 MeV to be negative and tentatively assign them J^π values of $\frac{5}{2}^-$ and $\frac{7}{2}^-$, respectively. We also confirm prior J^π assignments of $\frac{11}{2}^-$ and $\frac{9}{2}^-$, respectively, for the levels at 7.76 and 9.15 MeV. Our new J^π assignments for the levels at 6.86, 6.97, 7.58, and 8.47 MeV disagree with those suggested previously.[1]

Our measurements confirm the existence of a narrow level at 8.90 ± 0.02 MeV that was first reported more than two decades ago.[39] We tentatively assign $J^\pi = \frac{9}{2}^-$ to this level. This level and the $\frac{7}{2}^-$ state at 8.97 MeV

are assumed to be dominated by the predominantly 4p-3h weak-coupling configuration $1p_{1/2} \otimes {}^{16}O(4^+)$, where $^{16}O(4^+)$ denotes the predominantly 4p-4h state in ^{16}O at 10.36 MeV. We also report a new narrow level at 12.22 ± 0.02 MeV and confirm the existence of a $\frac{9}{2}^-$ state with $T = \frac{3}{2}$ at 14.72 ± 0.02 MeV. The 14.72-MeV state corresponds to the narrow state recently reported at 14.75 MeV in an electron-scattering experiment at low momentum transfer.[7]

We propose the existence of a predominantly 5p-4h rotational band in ^{17}O, which contains the levels at 5.87, 6.86, 7.58, and 8.47 MeV. All four levels have narrow widths ($\Gamma \leq 2$ keV) and are strongly excited by electric quadrupole transitions. Similar positive-parity rotational bands are known to exist in ^{16}O and ^{18}O. For example, the 0^+, 2^+, and 4^+ levels in ^{16}O at 6.05, 6.92, and 10.36 belong to a predominantly 4p-4h rotational band and the 0^+, 2^+, and 4^+ levels in ^{18}O at 3.63, 5.26, and 7.12 MeV belong to a predominantly 4p-2h rotational band. The measured form factors for all these collective states have negligible transverse components.

Simple interpretations of many states are given within the framework of the weak-coupling model. An extensive phenomenological analysis was performed for most of the observed states below 9.5 MeV. Separations of the longitudinal and transverse form factors were performed and reduced transition probabilities were extracted. The present high-resolution electron-scattering work confirms the essential validity of the weak-coupling model for describing the nuclear structure of ^{17}O.

ACKNOWLEDGMENTS

[a]Mailing address: Department of Physics, Kent State University, Kent, OH 44242.

[b]Present address: Harris Semiconductor, Mail Stop 51-180, Melbourne, FL 32901.

[c]Present address: Department of Physics, College of William and Mary, Williamsburg, VA 23185.

[d]Present address: Department of Physics, University of New Hampshire, Durham, NH 03824.

[e]Present address: Department of Physics, University of Washington, Seattle, WA 98195.

[f]Present address: Los Alamos National Laboratory, Los Alamos, NM 87545.

[g]Present address: Department of Physics and Astronomy, University of Maryland, College Park, MD 20742.

[h]Present address: Department of Physics, University of Kentucky, Lexington, KY 40506.

[i]Present address: Tektronics Inc., Beaverton, OR 97077.

[j]Present address: Department of Physics, University of Virginia, Charlottesville, VA 22901.

[k]Retired.

[1]F. Ajzenberg-Selove, Nucl. Phys. A375, 1 (1982).

[2]H. B. Burrows, W. M. Gibson, and J. Rotblat, Phys. Rev. 80, 1095 (1950); S. T. Butler, ibid. 80, 1095 (1950).

[3]T. L. Alexander, C. Broude, and A. E. Litherland, Nucl. Phys. 53, 593 (1964).

[4]R. G. Johnson, B. L. Berman, K. G. McNeil, J. G. Woodworth, and J. W. Jury, Phys. Rev. C 20, 27 (1979).

[5]J. C. Kim, R. Yen, I. P. Auer, and H. S. Caplan, Phys. Lett. 57B, 341 (1975); J. C. Kim, R. S. Hicks, R. Yen, I. P. Auer, H. S. Caplan, and J. C. Bergstrom, Nucl. Phys. A297, 301 (1978).

[6]B. E. Norum, J. C. Bergstrom, and H. S. Caplan, Nucl. Phys. A289, 275 (1977).

[7]C. Rangacharyulu, E. J. Ansaldo, D. Bender, A. Richter, and E. Spamer, Nucl. Phys. A406, 493 (1983).

[8]D. M. Manley, B. L. Berman, W. Bertozzi, J. M. Finn, F. W. Hersman, C. E. Hyde-Wright, M. V. Hynes, J. Kelly, M. A. Kovash, S. Kowalski, R. W. Lourie, B. Murdock, B. E. Norum, B. Pugh, and C. P. Sargent, Phys. Rev. C 34, 1214 (1986).

[9]H. Miska, B. Norum, M. V. Hynes, W. Bertozzi, S. Kowalski, F. N. Rad, C. P. Sargent, T. Sasanuma, and B. L. Berman, Phys. Lett. 83B, 165 (1979); M. V. Hynes, H. Miska, B. Norum, W. Bertozzi, S. Kowalski, F. N. Rad, C. P. Sargent, T. Sasanuma, W. Turchinetz, and B. L. Berman, Phys. Rev. Lett. 42, 1444 (1979).

[10]T. N. Buti, J. Kelly, W. Bertozzi, J. M. Finn, F. W. Hersman, C. Hyde-Wright, M. V. Hynes, M. A. Kovash, S. Kowalski, R. W. Lourie, B. Murdock, B. E. Norum, B. Pugh, C. P. Sargent, W. Turchinetz, and B. L. Berman, Phys. Rev. C 33, 755 (1986).

[11]C. E. Hyde-Wright, W. Bertozzi, T. N. Buti, J. M. Finn, F. W. Hersman, M. V. Hynes, M. A. Kovash, J. J. Kelly, S. Kowalski, J. Lichtenstadt, R. W. Lourie, B. E. Norum, B. Pugh, C. P. Sargent, B. L. Berman, F. Petrovich, and J. A. Carr, Phys. Rev. C 35, 880 (1987); C. E. Hyde-Wright, Ph.D. thesis, Massachusetts Institute of Technology, 1984.

[12]B. E. Norum, M. V. Hynes, H. Miska, W. Bertozzi, J. Kelly, S. Kowalski, F. N. Rad, C. P. Sargent, T. Sasanuma, W. Turchinetz, and B. L. Berman, Phys. Rev. C 25, 1778 (1982).

[13]W. Bertozzi, M. V. Hynes, C. P. Sargent, C. Creswell, P. C. Dunn, A. Hirsch, M. Leitch, B. Norum, F. N. Rad, and T. Sasunuma, Nucl. Instrum. Methods 141, 457 (1977); W. Bertozzi, M. V. Hynes, C. P. Sargent, W. Turchinetz, and C. Williamson, ibid. 162, 211 (1979).

[14]R. H. Condit, W. H. Parrish, Sr., and W. E. Sunderland (unpublished).

[15]J. Kelly, computer code ALLFIT (unpublished).

[16]L. W. Mo and Y. S. Tsai, Rev. Mod. Phys. 41, 205 (1969).

[17]J. Bergstrom, in Medium Energy Nuclear Physics with Elec-

tron Linear Accelerators, MIT, 1967, U.S. Dept. of Commerce Technical Information Note TID-24667 (U.S. GPO, Washington, D.C., 1967), p. 251.

[18]C. Creswell, LNS-MIT Internal Report No. 761, 1976.

[19]T. DeForest, Jr. and J. D. Walecka, Adv. Phys. **15**, 1 (1966).

[20]See, for example, R. S. Willey, Nucl. Phys. **40**, 529 (1963).

[21]B. A. Brown, B. H. Wildenthal, C. F. Williamson, F. N. Rad, S. Kowalski, H. Crannell, and J. T. O'Brien, Phys. Rev. C **32**, 1127 (1985).

[22]T. W. Donnelly and W. C. Haxton, At. Data Nucl. Data Tables **23**, 103 (1979).

[23]R. Bansal and J. B. French, Phys. Lett. **11**, 145 (1964).

[24]L. Zamick, Phys. Lett. **19**, 580 (1965).

[25]R. Sherr, R. Kouzes, and R. Del Vecchio, Phys. Lett. **52B**, 401 (1974).

[26]A. H. Wapstra and K. Bos, At. Data Nucl. Data Tables **19**, 177 (1977).

[27]A. Arima, H. Horiuchi, and T. Sebe, Phys. Lett. **24B**, 129 (1967).

[28]G. E. Brown and A. M. Green, Nucl. Phys. **75**, 401 (1966); **85**, 87 (1966).

[29]A. P. Zuker, B. Buck, and J. B. McCrory, Phys. Rev. Lett. **21**, 39 (1968); Brookhaven National Laboratory Informal Report No. BNL-14085, 1969 (unpublished).

[30]P. J. Ellis and T. Engeland, Nucl. Phys. **A144**, 161 (1970); T. Engeland and P. J. Ellis, *ibid.* **A181**, 368 (1972).

[31]B. S. Reehal and B. H. Wildenthal, Part. Nuclei **6**, 137 (1973).

[32]J. B. Flanz, R. S. Hicks, R. A. Lindgren, G. A. Peterson, A. Hotta, B. Parker, and R. C. York, Phys. Rev. Lett. **41**, 1642 (1978).

[33]J. Birkholz and F. Beck, Phys. Lett. **28B**, 18 (1968).

[34]M.-C. Lemaire, M. C. Mermaz, and K. K. Seth, Phys. Rev. C **5**, 328 (1972).

[35]K. Bethge, D. J. Pullen, and R. Middleton, Phys. Rev. C **2**, 395 (1970).

[36]D. Lister and A. Sayres, Phys. Rev. **143**, 745 (1966).

[37]C. H. Johnson, Phys. Rev. C **7**, 561 (1973); **8**, 851(E) (1973); J. L. Fowler, C. H. Johnson, and R. M. Feezel, *ibid.* **8**, 545 (1973).

[38]R. B. Walton, J. D. Clement, and F. Boreli, Phys. Rev. **107**, 1065 (1957).

[39]B. K. Barnes, T. A. Belote, and J. R. Risser, Phys. Rev. **140**, B616 (1965).

[40]G. W. Kerr, J. M. Morris, and J. R. Risser, Nucl. Phys. **A110**, 637 (1968).

[41]H. Schmidt-Böcking, G. Brommundt, and K. Bethge, Z. Phys. **246**, 431 (1971).

[42]M. J. Smithson, D. L. Watson, and H. T. Fortune, J. Phys. G **12**, 985 (1986).

[43]J. L. Groh, R. P. Singhal, H. S. Caplan, and B. S. Dolbilkin, Can. J. Phys. **49**, 2743 (1971).

[44]B. A. Brown, A. Etchegoyen, W. D. M. Rae, and N. S. Godwin, Computer Code OXBASH (unpublished).

[45]C. L. Blilie, D. Dehnhard, M. A. Franey, D. H. Gay, D. B. Holtkamp, S. J. Seestrom-Morris, P. J. Ellis, C. L. Morris, and D. J. Millener, Phys. Rev. C **30**, 1989 (1984).

[46]B. G. Harvey, J. Cerny, R. H. Pehl, and E. Rivet, Nucl. Phys. **39**, 160 (1962); C. C. Lu, M. S. Zisman, and B. G. Harvey, Phys. Rev. **186**, 1086 (1969).

[47]F. A. Rose, Nucl. Phys. **A124**, 305 (1969).

[48]F. Ajzenberg-Selove, Nucl. Phys. **A166**, 1 (1971).

[49]M. E. Clark, K. W. Kemper, and J. D. Fox, Phys. Rev. C **18**, 1262 (1978).

[50]K. T. Knöpfle, P. Doll, H. Breuer, and G. J. Wagner, Nucl. Phys. **A280**, 97 (1977).

[51]W. L. Baker, C. E. Busch, J. A. Keane, and T. R. Donoghue, Phys. Rev. C **3**, 494 (1971).

[52]J. Bobker, Phys. Rev. **185**, 1294 (1969).

[53]See, for example, B. Margolis and N. de Takacsy, Can. J. Phys. **44**, 1431 (1966); M. Harvey, Phys. Lett. **3**, 209 (1963).

[54]S. Cierjacks, F. Hinterberger, G. Schmalz, D. Erbe, P. V. Rossen, and B. Leugers, Nucl. Instrum. Methods **169**, 185 (1980).

[55]F. Hinterberger, P. Von Rossen, S. Cierjacks, G. Schmaltz, D. Erbe, and B. Leugers, Nucl. Phys. **A352**, 93 (1981).

[56]See AIP Document PRVC-36-1700-48 for 48 pages containing a complete tabulation of the data described in this paper. Order by PAPS number and journel reference from American Institute of Physics, Physics Auxuliary Publication Service, 335 E. 45 St., New York, NY 10017. The price is $1.50 for each microfiche or $5.00 for photocopies of up to 30 pages and $0.15 for each page over 30 pages. Airmail additional. Make checks payable to American Institute of Physics.